University of Alberta

Remote Sensing and Analysis of Forest Environments

by

Mark Alexander Kachmar

©

A thesis submitted to the Faculty of Graduate Studies and Research in partial fulfillment of the requirements for the degree of Master of Science

Department of Earth and Atmospheric Sciences

Edmonton, Alberta
Spring, 2004

Library and Archives Canada
Published Heritage Branch
395 Wellington Street
Ottawa ON K1A 0N4
Canada

Bibliothèque et Archives Canada
Direction du Patrimoine de l'édition
395, rue Wellington
Ottawa ON K1A 0N4
Canada

Your file Votre référence
ISBN: 0-612-96497-3
Our file Notre référence
ISBN: 0-612-96497-3

The author has granted a non-exclusive license allowing the Library and Archives Canada to reproduce, loan, distribute or sell copies of this thesis in microform, paper or electronic formats.

The author retains ownership of the copyright in this thesis. Neither the thesis nor substantial extracts from it may be printed or otherwise reproduced without the author's permission.

L'auteur a accordé une licence non exclusive permettant à la Bibliothèque et Archives Canada de reproduire, prêter, distribuer ou vendre des copies de cette thèse sous la forme de microfiche/film, de reproduction sur papier ou sur format électronique.

L'auteur conserve la propriété du droit d'auteur qui protège cette thèse. Ni la thèse ni des extraits substantiels de celle-ci ne doivent être imprimés ou aturement reproduits sans son autorisation.

In compliance with the Canadian Privacy Act some supporting forms may have been removed from this thesis.

While these forms may be included in the document page count, their removal does not represent any loss of content from the thesis.

Conformément à la loi canadienne sur la protection de la vie privée, quelques formulaires secondaires ont été enlevés de cette thèse.

Bien que ces formulaires aient inclus dans la pagination, il n'y aura aucun contenu manquant.

Canada

ABSTRACT

High and medium resolution multispectral satellite imagery is used to classify live post-fire forest residuals within two large forest fire affected areas (> 100,000 ha) in the northern boreal forest of Alberta, Canada. Residual forest patches are converted to polygons to calculate patch and shape metrics at nine minimum mapping unit classes. Results are analyzed and compared within and between the two fires. Results indicate how sensor spatial resolution, choice of MMU and anthropogenic features (i.e. highways, transmission lines) affect post fire residual patch and shape level metrics.

The spectral angle mapper (SAM) classifier is used to classify forest cover on a highly industrialized mountain region in the central part of Honshu, Japan using Landsat TM 5 satellite imagery. Research findings relate land use and cover change (LUCC) processes on the mountain to image classification challenges. Findings illustrate the importance of calculating the spectral separability between forest cover types when developing a forest cover classification scheme in mountain regions where forest cover has been anthropogenically modified.

ACKNOWLEDGEMENTS

I would like to thank my supervisors Dr. G. Arturo Sánchez-Azofeifa and Dr. Benoit Rivard for providing me with the support and tools necessary to conduct my research. I am grateful to Dr. Sanchez for providing me with experiences to participate in his international research opportunities that have helped me gain a great deal of practical field and laboratory experience. His feedback on proposals and manuscripts helped to improve the quality of the thesis and my degree program in general. I wish to thank Dr. Rivard for providing guidance and feedback on research proposals and manuscripts drafts during the course of my studies. I thank him also for providing valuable career development advice during my studies. Thanks to external committee member Dr. Terry Caelli for reviewing and proving comments to my thesis.

Thank you to Prof. Dr. Yoshitaka Kakubari at the Department of Forestry and Silviculture at Shizuoka University, Japan, for his help in supporting the Mt. Naeba research study.

I would like to acknowledge the Sustainable Forestry Management Network (SFMN) and Mr. Bruce Macnab for helping facilitate my internship with ALPAC as well as supporting my research at various SFMN events. Thanks to Dr. Elston Dzus for facilitating my industrial fellowship at Alberta Pacific Forestry Industries Inc. (ALPAC) and to Mr. Matthew Smith (ALPAC) for valuable discussions that allowed me to develop our research study. Thanks also the Environmental Science team at ALPAC for the opportunity to present my research and to Vince Eggleston who provided feedback on many questions about residual harvesting practices in Alberta.

Thanks to the American Society for Photogrammetry and Remote Sensing and the Space Imaging corporation for providing me with the Space Imaging award that allowed me to process the satellite image for one of my study areas.

Thanks to Tomás de Camino Beck and Steven Hamilton for valuable discussions and critical feedback during the course of my degree. I also wish to acknowledge the Earth Observation Systems Laboratory Land use and cover change (LUCC) research group for the opportunity to present research papers and ideas. Thanks to Patrick van Laake and Dr. Jinkai Zhang for their Remote Sensing and GIS expertise. I would like to thank Dr. Jilu Feng for his help with IDL programming. Thanks to Shasta Rudyk for helping with fieldwork at the Crow Lake Ecological Reserve.

I thank also visiting Prof. Sawagaki for helping organize the Japanese data conversion programs and Larissa Kachmar for her help in developing presentations and poster ideas. Thanks to Josh Evans and Jeff Masuda and the Human Geography Society (HuGs) for providing the framework for discussing geography related topics and to all my friends that took my mind away from the thesis when I needed it.

Finally, I thank my parents for their patience and support during the course of my studies.

TABLE OF CONTENTS

CHAPTER 1: INTRODUCTION 1

1.1 Introduction 1

1.2 Literature Cited 5

CHAPTER 2: DETECTION & ANALYSIS OF POST-FIRE RESIDUALS USING MEDIUM AND HIGH RESOLUTION SATELLITE IMAGERY 10

2.1 Introduction 10

2.2 Methodology 13

2.2.1 Study Areas & Data Sets 13

2.2.2 Image Preprocessing & Field Data Collection 15

2.2.3 Supervised Image Classification & Metric Calculations 16

2.3 Results & Discussion 18

2.3.1 Spectral Seperability & Accuracy Assessment 18

2.3.2 Patch & Shape Level Metrics 19

2.4 Conclusions 24

2.5 Literature Cited 26

CHAPTER 3: FOREST COVER CLASSIFICATION IN INDUSTRIALIZED MOUNTAIN TERRAIN USING LANDSAT TM 5 IMAGERY **46**

3.1 Introduction 46

3.2. Study area 49

3.2.1 Study area description 49

3.3 Methodology 51

3.3.1 Image Pre-processing 51

3.3.2 Field data collection 52

3.3.3 Training Area Selection & Spectral Separability 53

3.3.4 Supervised Spectral Angle Mapper [SAM] Classifier 54

3.4 Results & Discussion 55

3.4.1 Forest Cover Spectral Separability 55

3.4.2 Forest Classification Accuracy & Analysis 59

3.4.3 Implications for Regional Monitoring Systems 61

3.5 Conclusion 63

3.6 Literature Cited 64

CHAPTER 4: SUMMARY AND CONCLUSIONS **79**

4.1 Summary & Conclusions 79

4.2 Recommendations 81

LIST OF TABLES

CHAPTER 2

Table 2.1 Residual forest patch metrics as a function of minimum mapping unit for the 2002 House River fire derived from a supervised maximum likelihood classification on a 4 m resolution IKONOS image. 33

Table 2.2 Residual forest patches metrics as a function of minimum mapping unit for the 2001 Chisholm Fire derived from a supervised maximum likelihood classification on a 28.5 m resolution Landsat ETM+ image. 33

CHAPTER 3

Table 3.1 Jeffries-Matusita distance calculated on the original and topographically corrected forest cover types over Mt. Naeba in the central part of Honshu, Japan. 70

Table 3.2 Error matrix for the land cover classes within the Mt. Naeba study area, Japan. 71

Table 3.3a Land cover type as a percentage of total land cover area within the study area. 72

Table 3.3b Land cover type as a percentage of total land cover area within the study area without topographic correction. 72

LIST OF FIGURES

CHAPTER 2

Figure 2.1 Oblique view of the locations and geometric shapes of unburnt [residual] forest patches that occur a) within fire perimeters and b) along transmission lines. 34

Figure 2.2 Location of the Crow Lake Ecological Reserve [affected by the 2002 House River fire] and the 2001 Chisholm Fire overlaid onto border of the Province of Alberta, Canada. 35

Figure 2.3 Outline of the 2001 Chisholm Fire perimeter represented by a 3-band image composite (bands 5 4 3) of the Landsat ETM+ image. Darker colors represent those areas burnt in the fire. Green colored areas represent live vegetation cover. The Landsat ETM+ image was subset from the original full image scene (Path 43 Row 22) and geo-rectified using a image to vector registration by selecting ground control points at key road intersection using 1: 20, 000 vector access data. The image was re-projected to Universal Transverse Mercator (UTM) Zone 11, NAD 83 for subsequent processing. 36

Figure 2.4 3-Band Image Composite (Bands 4 3 2) of the IKONOS image that was acquired over the House River fire on August 29, 2002. Red colored areas represent residual forest, while green color regions represent areas burnt by the fire. Crow Lake is located near the centre of the image. For the 2002 House Rive Fire, an IKONOS multispectral image was acquired over a 10 x 10 km area (Crow Lake Ecological Reserve). This image was re-projected to UTM Zone 12 and the boundary of the IKONOS scene formed the study area. 37

Figure 2.5 Flowchart outlining the methodological processes involved in detecting and analyzing residual forest cover using Landsat ETM+ and IKONOS imagery. 38

Figure 2.6 3-Dimensional visualization of training sites within the a) 2001 Chisholm and b) 2002 House River fires overlaid on Landsat ETM+ bands 543. 39

Figure 2.7 Total residual area calculated as a function of minimum mapping unit from a classified Landsat ETM+ image acquired over the perimeter of the 2001 Chisholm fire and from a classified IKONOS image acquired over the 2002 House River Fire. 40

Figure 2.8 Number of Patches and Mean Patch Size calculated as a function of minimum mapping unit for the perimeter of the 2001 Chisholm and 2002 House River Fires. 41

Figure 2.9 Bird's eye view of the effect of increasing sensor spatial resolution on different sized residual forest patches overlaid onto a grid representing sensor field of view at arbitrary 28.5, 15 and 4 - meter sensor spatial resolution. 42

Figure 2.10 Bird's-eye-view pictorial representation of the locations and geometric shapes of unburnt [residual] forest patches located within the Chisholm (2001) and House River (2002) fire perimeter occurring as a) isolated forest islands; b) between agricultural fields; c) bordering lakes; d) along seismic lines; e) along road edges; and f) along transmission lines. 43

Figure 2.11 Areal Weighted Mean Shape Index (AWMSI) calculated as a function of minimum mapping unit for the perimeter of the 2001 Chisholm and 2002 House River Fires. 44

Figure 2.12 Pictorial representation of the effect of increasing sensor spatial resolution on different sized residual forest patches affected by a) seismic lines; b) bordering lakes; and c) roads overlaid onto a grid representing sensor field of view at 28.5, 15 and 4 - metre sensor spatial resolution perimeter. 45

CHAPTER 3

Figure 3.1 Location of the study area, central part of Honshu, Japan. 73

Figure 3.2 Flowchart of the processes involved in pre-processing and classifying the Landsat TM image for Mt. Naeba in the Central part of Honshu, Japan. A cloud free 6-channel multispectral LANDSAT TM 5 (Path 108/ Row 34) image was acquired over Mt. Naeba in the central part of Honshu, Japan, on September 01, 1999, with a solar azimuth of 121° and angle elevation of 59 °. 74

Figure 3.3 a) Original LANDSAT TM 5 color composite (bands 543 as RGB) over Mt. Naeba and b) Topographically corrected 3-Band Image Composite (Bands 5 4 3) of the LANDSAT TM 5. 75

Figure 3.4 Two-dimensional scatter plot of training site spectral data for forest classes within the Mt. Naeba study area in the central part of Honshu, Japan a) pre topographic correction Birch Forest (Yellow), Beech (Green), Cedar (Red), Mix Deciduous (Cyan) & b) post topographic correction. Spectral data displayed in Landsat TM bands 4 & 5. 76

Figure 3.5 N-Dimensional Visualization of training site spectral data for the classes of interest within the Mt. Naeba study area in the central part of Honshu,

Japan a) and c) pre topographic correction & b) and d) post topographic correction. Birch (Yellow), Beech (Green), Cedar (Red), Mix Deciduous (Cyan). Displayed axes refer to Landsat TM bands. 77

Figure 3.6 Spectral angle mapper (SAM) classification of the Landsat TM image acquired over Mt. Naeba in the Central part of Honshu, Japan. 78

LIST OF SYMBOLS

AWMSI	*Areal Weighted Mean Shape Index*
CA	*Class Area*
DEM	*Digital Elevation Model*
DN	*Digital Number*
ETM+	*Enhanced Thematic Mapper Plus*
FOV	*Field-of-view*
GIS	*Geographic Information Systems*
GPS	*Global Positioning Systems*
JM	*Jeffries Matusita*
LC	*Land Cover*
LU	*Land Use*
LUCC	*Land use and cover change*
MMU	*Minimum Mapping Unit*
MPS	*Mean Patch Size*
NIR	*Near Infrared*
NDVI	*Normalized Difference Vegetation Index*
NumP	*Number of Patches*
RMSE	*Root Mean Square Error*

RS	*Remote Sensing*
SAM	*Spectral Angle Mapper*
SWIR	*Short Wave Infrared*
TM	*Thematic Mapper*
UTM	*Universal Transverse Mercator*
VIS	*Visible*
VNIR	*Visible Near infrared*

CHAPTER 1

1.1 INTRODUCTION

Significant global changes to biodiversity, productivity, migration and sustainability of earth's natural resources are affecting the present and future social, economic and political stability of human society (Dale, 1997, Lambin *et al.*, 2001). To effectively deal with these global changes, geographers, land managers, foresters, biologists and environmentalists will require timely and accurate local and global scale land cover information (Vogelmann *et al.*, 2001). With the capability of acquiring synoptic coverage over large areas, spaceborne satellite imagery provides both a timely and practical means for monitoring land cover that can form a useful framework from which to initiate long term land cover mapping and monitoring (Cihlar, 2000; Masek *et al.*, 2001; Rogan *et al.*, 2002). Continuing improvements in imaging sensor capabilities, decreased costs of image acquisition, due to competition among data providers, in combination with a large suite of commercial image processing and geographic information software, are also leading to wider and unprecedented uses of satellite imagery for natural resource management applications (ASPRS, 2002). The secondary spatial data products that can be derived from satellite imagery, including classified image products, Geographic Information System (GIS) layers or tabular/statistical data allow for further insight and analysis into regional and global land use and land cover change (LUCC) processes (IPCC, 2000; Briassoulis, 2001). Land cover refers to the biophysical attribute of the land surface (i.e.

beech forest) and land use refers to the human processes that the land is being used for (Nunes & Augé, 2003). Satellite imagery is thus becoming a mainstream and routine tool in academic, government and industrial projects concerned with mapping and monitoring land cover changes (Cihlar, 2000; Martinez-Casasnovas, 2000; Franklin & Wulder, 2002)

However, due to the challenge of accurately classifying forest cover (Foody, 2000; Woodcock *et al.*, 2001), many new and emerging technologies, methods and techniques are evolving and continually being tested and debated by the remote sensing community. Forest cover classification challenges via remote sensing arise from the dynamic nature of forest ecosystems across both spatial and temporal scales (Bonan & Shugart, 1989). Over time the age, structure, composition, and spatial patterns of forest cover change as a forest grows and develops toward a mature ecosystem (i.e. forest succession). Additionally, those areas affected by a physical disturbance such as a forest fire, or forest harvesting, may exhibit a high degree of forest canopy heterogeneity and structural complexity, depending on the severity and extent of these disturbances. In these dynamic industrialized areas, the process of defining what actually constitutes a forest becomes a matter of debate (Bennet, 2001).

The remote sensing and forestry community have placed much emphasis on interpreting forest cover from satellite images using various image classification techniques (Ichoku *et al.*, 1996; Bastin, 1997; Foody, 2000) and then attempting to validate the accuracy of the classification (Congalton, 1991; Stehman & Czaplewski, 1998). Only recently have remote sensing based studies began examining the dependence

of forest classification accuracy on the spatial locations and patterns of the forest cover types within an image scene (Smith, 2002; King, 2002) or even the size of the forest stands (Hyyppä & Hyyppä, 2001) in relation to the capabilities of the imaging sensor.

The main objective of this thesis is to classify and examine forest cover using medium (i.e. LANDSAT TM & ETM+) and high-resolution (i.e. IKONOS) satellite imagery acquired over forested areas affected by both natural (i.e. fire) and anthropogenic (i.e. harvesting) processes. The thesis has been organized into the following chapters:

Chapter 2: Detection and Analysis of Post-Fire Residuals Using Medium and High Resolution Satellite Imagery

Although forest fires can burn over large areas over short time periods, forest fires rarely consume everything in their path. They tend to leave behind live irregularly shaped patches and/or linear rows of mature trees (i.e. residuals) within the fire perimeter. This chapter uses high [IKONOS] and medium resolution [Landsat Enhanced Thematic Mapper Plus ETM+] multispectral satellite imagery and a hybrid unsupervised [image-masking] and supervised classification technique, to classify forest residuals within two large forest fire affected areas (> 100,000 ha) in the northern boreal forest of Alberta, Canada. Residual patches are then converted to polygons to calculate patch and shape metrics at multiple minimum mapping unit (MMU) classes. Results are then analyzed and compared within and between the two fires. Results analyzed and compared within and between the two fires indicate how the choice of satellite imagery, MMU and degree

of linear disturbances (i.e. highways, transmission/seismic lines) affect the interpretations of residual patches and shapes within fire perimeters. The results of this study serve as an important guideline for the use of data derived from remote sensing platforms into residual retention forest harvesting protocols that aim to base forest harvesting practices on emulating fire in the landscape (*Proposed submission to the Canadian Journal of Forest Research*).

Chapter 3: Forest Cover Classification in Industrialized Mountain Terrain Using Landsat TM 5 Imagery

Forest cover classification using satellite imagery is complicated in highly mountainous terrain by the impacts of topographic shading, but land use and land cover change (LUCC) processes that disturb the forest environment also have an impact. These disturbances alter the structure of the various forest cover types, affecting the spectral reflectance properties they exhibit. Landsat TM 5 satellite imagery is used to characterize forest cover types in a highly industrialized ski resort [Naeba Mountains] in the central part of Honshu, Japan. Training areas representing the forest cover types are identified in the field and Jeffries-Matusita distance is used to calculate the separability between these training areas. The forest cover types are then classified using a supervised spectral angle mapper classifier (SAM). Research findings highlight the importance of accounting for not only topographical shadowing effects, but also the impacts of human induced land use changes (i.e. forest harvesting, thinning) practices when attempting to select training

areas to characterize forest cover in industrialized mountainous areas *(Proposed submission to the Journal of Mountain Research & Development).*

Chapter 4: Summary, Conclusions and Recommendations

The aim of this thesis is to examine and analyze forest cover using satellite imagery. In the final chapter of this thesis the major conclusions of the chapters two and three are reviewed and a number of recommendations for the use of remote sensing in forest cover monitoring and mapping are provided. This chapter provides recommendation to those end users from the fields of environmental science, geography and biology that will ultimately use the secondary spatial data products derived from such imagery (i.e. image classification) for ecosystem management. It is noted that without an understanding of how the final land cover classification products have been generated, the effectiveness of using the data products to support natural resource management, conservation or habitat studies may be limited.

1.2 LITERATURE CITED

ASPRS. 2002. American Society for Photogrammetric Engineering and Remote Sensing Internal Publication. Washington, D.C.

Bastin, L. 1997. Comparison of fuzzy c-means classification, linear mixture modelling and MLC probabilities as tools for unmixing coarse pixels. *International Journal of Remote Sensing,* 18 (17), 3629-3648.

Bennet, B. 2001. What is a Forest? On the Vagueness of Certain Geographical Concepts. *Topoi,* 20, 189-201.

Bonan, G.H. & Shugart, H.H.. 1989. Environmental Factors and Ecological Processes in Boreal Forests. *Annual Review of Ecology and Systematics*, 20, 1-28.

Briassoulis, H. 2001. Policy-Oriented Integrated Analysis of Land-Use Change: An Analysis of Data Needs. *Environmental Management*, 27 (1), 1-11.

Cihlar, J. 2000. Land cover mapping of large areas from satellites: status and research priorities. *International Journal of Remote Sensing, 21* (6,7), 1093-1114.

Congalton, R. G. 1991. A Review of Assessing the Accuracy of Classifications of Remotely Sensed Data. *Remote Sensing of Environment,* 7, 35-46.

Dale, V. 1997. The relationship between land-use change and climate change. *Ecological Applications,* 7 (3), 753-769.

Foody, G. M. 2000. Estimation of sub-pixel land cover composition in the presence of untrained classes. *Computers & Geosciences,* 26, 469-478.

Franklin, S. & Wulder, M. 2002. Remote sensing methods in medium spatial resolution satellite data land cover classification of large areas. *Progress in Physical Geography*, 26 (2), 173-205.

Hyyppä, H , Hyyppä, J., 2001. Effects of stand size on the accuracy of remote sensing-based forest inventory. *IEEE Transaction on Geoscience and Remote Sensing,* 39(12), 2613-2621.

Ichoku, C. K., A. 1996. A Review of Mixture Modelling Techniques for Sub-Pixel Land Cover Estimation. *Remote Sensing Reviews,* 13, 161-186.

Intergovernmental Panel on Climate Change [IPCC] (2000). Land Use, Land-Use Change, and Forestry. Cambridge University Press (377 pp).

King, R.B. 2002. Land cover mapping principles: a return to interpretation fundamentals. *International Journal of Remote Sensing*, 23 (18), 3524-3545.

Lambin, E.F, Turner, B.L., Geist, H.J., Agbola, S.B., Angelsen, A., Bruce,.J.W., Coomes, O.T., Dirzo, R., Fischer, G., Folke, C., George, P.S., Homewood, K., Imbernon, J., Lemans, R., Li, X., Moran, E., Mortimer, M., Ramakrishna, P.S., Richards,

J.F., Scans, H., Steffen, W., Stone, G.D., Sedan, U., Beldam, T.A., Vogel, C. & Up, J. 2001. The causes of land-use and land-cover change: moving beyond the myths. *Global Environmental Change*, 11, 261-269.

Martinez-Casasnovas, J. 2000. A Cartographic and database approach for land cover/use mapping and generalization from remotely sensed data. *International Journal of Remote Sensing*, 21 (9), 1825-1842.

Masek, J. G., Honzak, M., Goward, S.N., Liu, P. 7 Pak, E. 2001. Landsat-7 ETM+ as an observatory for land cover: Initial radiometric and geometric comparisons with Landsat-5 Thematic Mapper. *Remote Sensing of Environment,* 78, 118-130.

Nunes, C. & Augé, J.I. (Eds) 1999. Land-Use and Land-Cover Change (LUCC) Implementation Strategy. *LUCC Report Series 48.* IGBP Secretariat, Stockholm, 125 pp.

Rogan, J., Franklin, J. & Roberts, D.A. 2002. A Comparison of methods for monitoring multitemporal vegetation change using Thematic Mapper Imagery. *Remote Sensing of Environment,* 80, 143-156.

Smith, J., Wickham, J.D., Stehman, S.V., & Yang, L. 2002. Impacts of Patch Size and Land-Cover Heterogeneity on Thematic Image Classification Accuracy. *Photogrammetric Engineering & Remote Sensing,* 68(1), 65-70.

Stehman, S.V. & Czaplewski, R.L., 1998. Design and Analysis for Thematic Map Accuracy Assessment: Fundamental Principles. *Remote Sensing of Environment*, 64, 331-344.

Vogelmann, J. E., Helder, D., Morfitt, R., Choate, M.J., Merchant, J.W., Bulley, H. 2001. Effects of Landsat 5 Thematic Mapper and Landsat 7 Enhanced Thematic Mapper Plus radiometric and geometric calibrations and corrections on landscape characterization. *Remote Sensing of Environment,* 78, 55-70.

Woodcock, C. E., Macomber, S.A., Pax-Lenney, M. & Cohen, W.B. 2001. Monitoring large areas for forest change using Landsat: Generalization across space, time and Landsat sensors. *Remote Sensing of Environment,* 78, 194-203.

CHAPTER 2

DETECTION AND ANALYSIS OF POST FIRE RESIDUALS USING HIGH AND MEDIUM RESOLUTION SATELLITE IMAGERY

2.1 INTRODUCTION

Each year approximately 5000-12,000 forest fires covering roughly 1-3 million hectares burn across areas of Canada (Amiro *et al.*, 2001). In boreal regions, these fires can affect large areas relatively quickly (Martell, 2001) including peat lands (Kuhry, 1994). However the destructive capability of such fires (i.e. fire severity) is not constant across the landscape and is instead modified by local weather, topography and pre-fire vegetation types at the time of burning (Sousa, 1984; Bonan & Shugart, 1989). These forest fires rarely consume everything in their path and tend to leave behind live irregularly shaped patches and/or linear rows of mature trees (i.e. residuals) within the fire perimeter (Rowe & Scotter, 1973) (Figure 2.1).

Residuals are economically and ecologically significant in boreal forest environments. Previous post-fire research has shown that residuals may comprise as much as three to fifteen percent of the vegetation cover within fire-affected areas (Delong & Kessler, 2000) and the total number of residual patches increases proportionally to the size of the fire perimeter (Eberhart & Woodard, 1987). Identifying and locating post-fire residuals is critical for foresters conducting post-fire site evaluations (Eberhart & Woodard, 1987) and for aiding in tree regeneration (Green *et al.*, 1999) and protecting bird habitat

(Schieck & Hobson, 2000). From a policy perspective, information on post fire residuals can be used at a local scale for establishing guidelines for devising forest harvesting practices that are based on emulating fire patterns (i.e. residual-retention harvesting) (Lee *et. al.*, 2002). Such information can also aid forestry companies harvest burnt trees from within the fire perimeter (i.e. salvage logging operations). At a national scale, information on the area and number of residuals can improve estimates of forest area burnt and provide key input for forest fuel mapping (Conard *et al.*, 2001; Sandberg *et al.*, 2001), carbon (Amiro *et al.*, 2001) and fire modelling databases (Keane *et al.*, 2001).

Various approaches exist for characterizing post fire land cover. Currently within Canada, government agencies map the perimeter of fire-affected and define large area residual forest stands using a helicopter equipped with an onboard global positioning unit or alternately rely on acquiring and interpreting residual stands using aerial photography (Amiro & Chen, 2003). However, in the case of large area fires (>100,000 ha) where numerous aerial photographs may be needed, manual photo-interpretation can be laborious as well as affected by the skill of the photo-interpreter (Strand *et al.*, 2002). The large area synoptic coverage provided by medium and high-resolution satellite imagery can provide a useful means to examine and characterize fire-affected areas (Pereira & Setzer, 1993; White *et al.*1996; Sunar & Özkan, 2001). However, rather than using this imagery to detect and analyze residual forest islands, satellite imagery is typically used to assess post fire regeneration (Riaño *et al.*, 2002) or define the fire affected portions of the image scene (Fraser *et al.*, 2001; Sunar & Özkan, 2001; Bougeau-Chavez *et al.*, 2002). This usually involves acquiring images taken before and after the fire (Rogan & Yool,

2001; Miller & Yool, 2002) or using normalized difference vegetation index (NDVI) methods (Garcia-Haro *et al.*, 2001) to define the fire perimeters.

Various explanations can be provided for the lack of studies using satellite imagery to detect and analyze post-fire residuals. The first is the human context that often dictates what will be considered in the final legend of a land cover classification (Harley, 1989; Dorling, 1998). For example, if the economic and ecological significance of residual forest patches are not known, it is likely that these patches will not be mapped or considered in the legend of a final classification scheme. The second reason may relate to the dynamic post-fire landscapes that fires create (Martell, 2001). For example, areas subject to a rapid physical disturbance such as a forest fire, can exhibit marked variation in the severity and extent of these disturbances that can lead to a high degree of forest canopy heterogeneity over space and time. The timing of image acquisition following a fire is also critical when attempting to detect residuals, considering the rapid increase of vegetation that recolonizes a fire site following the initial disturbance (Larson, 1980; White *et al.*, 1996; Diaz-Delgado *et al.*, 2003). Residuals can also maintain various shapes and sizes on the land base, and these are further modified by anthropogenic features (i.e. seismic lines, roads, transmission lines). The result being that spaceborne residual detection needs to be optimized with an imaging sensor that can resolve these unburnt forest patches from the surrounding burnt areas.

This research chapter employs medium and high-resolution IKONOS (4-m spatial resolution) and Landsat ETM+ (28.5 m spatial resolution) satellite imagery to detect and

analyze the distributions of live post-fire residuals within two large area (> 100, 000 ha) fires that occurred in Northern Alberta (Figure 2.2). This study differs from previous approaches to characterize fire-affected areas using satellite imagery by focusing not on what the fire consumed but on detecting those forest patches that remained alive within the fire perimeter. Residual patch and shape level metrics are calculated to examine how the choice of satellite imaging sensor, minimum mapping unit and anthropogenic features influence residual area statistics, which has implications for the use of residual data in post-fire burn mapping and residual retention forest harvesting.

2.2 METHODOLOGY

2.2.1 Study Areas & Data Sets

We examine two large area (>100,00 ha) fires [2001 Chisholm and 2002 House River] in Northern Alberta, Canada (Figures 2.3 & 2.4). The Chisholm fire ignited on May 23, 2001, near the hamlet of Chisholm, Alberta, and was estimated at over 116, 000 hectares. The forest industry lost 4.5 million cubic metres of growing stock and over 6, 300 ha of harvesting units (i.e. cutblocks) in varying stages of forest regeneration (Chisholm Fire Review Committee Final Report, 2001). The primary image data source for the study of this fire is a cloud free Landsat Enhanced Thematic Mapper Plus (ETM+) multispectral image (Path 43 Row22) acquired on 23 September 2001, approximately four months following the fire.

The House River Fire burned over 248 000 hectares in May 2002, forcing the evacuation of the communities of Conklin, Sandy Lake, Keg River, Peerless Lake, Trout Lake, Fox Lake and the Sunchild Indian Reserve (Chisholm Fire Review Committee Final Report, 2001). A multispectral IKONOS image (4 m spatial resolution) was acquired on August 29, 2002, approximately three months after the fire at the Crow Lake Ecological Reserve (centered at 112.10° W, 55.78° N), which is an area affected by the 2002 House River fire.

Both the 2001 Chisholm and the 2002 House River fires occurred within the Boreal forest region described by Rowe & Scotter (1973). Strong and Leggat (1981) provide a description of the physiography and climate of the study areas. Elevation ranges from less than 250m above sea level in the northeast to 1400 m in the southwest. Soils consist primarily of grey luvisols. Summer precipitation (May to September) varies from 180-440mm with maximum precipitation occurring in July. Dominant tree species found throughout this area include white spruce (*Picea glauca (Moench) Voss),* black spruce, *Picea mariana (Mil B.S.P.),* and trembling aspen *(Populus tremuloides Michx.).*

2.2.2 Image Preprocessing & Field Data Collection

The process of detecting and analyzing residuals in each of the study areas is outlined in the following flow diagram (Figure 2.5). Preliminary interpretation of the satellite images focused on identifying the major land cover types in both study area images (green residual areas, burnt areas, wetland and water bodies). Following this, each image was pre-processed into fifty spectral clusters using the ISODATA unsupervised classification (Tou & Gonzalez, 1974; Richards, 1994) to begin grouping the spectral classes into the relevant information classes. An atmospheric correction was not applied to the satellite images, because each scene was processed and classified independently (Song *et al.*, 2001). The fifty spectral classes were then grouped into ten information classes that included non-target (lakes, clouds, cloud shadows, haze, fire- affected areas, gravel pits, wetland areas) and target classes (residual areas). This resulted in an unsupervised classification map for each image that could be used to select areas that needed to be visited during the field campaign.

A field campaign was conducted during the summer 2002 (June-July-August) to identify green residuals areas and document major land cover types and spurious features within the study areas (Sánchez-Azofeifa *et al.*, 2003). To support data collection and map readability, both satellite images were printed at a 1:50,000 scale and overlaid with 1:20,000 scale vector access data (road, transmission lines, hydrological vectors). The presence of residuals were labeled on the field maps and recorded with a global positioning system unit. As salvage logging practices were taking place previous, during

and following the field campaign, validation information can only be verified for those residual areas viewed during the field campaign. For the 2001 Chisholm fire and 2002 House River fire study areas, 65 and 98 validation areas were selected, respectively.

Following the collection of residual field data, all non-vegetated land cover types in the satellite images (water bodies, clouds, cloud shadows) were eliminated from the scene by creating a series of image masks. Certain pixels adjacent to the clouds on the IKONOS image exhibited a small degree of class confusion and therefore minimal hand digitizing was required to correct this mis-classification. To create an output image that contained only vegetated and fire-affected cover types, the non-target features were masked out of the images. For each output image five homogeneous training sites, containing at least 500 image pixels (40 ha Chisholm Fire/0.8 ha House River fire) and representing two forest (deciduous and coniferous) and three wetland cover types were chosen in each of the study area images. Finally, spectral separability of the training areas was examined for both fires in *n*-dimensional image space. Although tree species would be useful information for forest management, such data collection and analysis was out of scope of the main goal of this chapter.

2.2.3 Supervised Image Classification & Metric Calculations

Training areas representing the given land cover classes identified in the field were input into a maximum likelihood supervised classifier (Richards, 1993) that generated a classification layer for each of the land cover types. Since the analysis focused only on

analyzing residual forest areas, all non-target classes were eliminated from this layer using a (1/0) mask. Finally, the residual-only layers were filtered using a 3x3 median filter to eliminate single pixels (Zukowskyj *et al.*, 2001). Validation data collected during the field campaign were used to assess the image classification accuracy of the residual forest areas. For this purpose (Congalton, 1991; Stehman & Czaplewski, 1998), sixty-five and ninety-eight validation areas were collected within the perimeter of the 2001 Chisholm Fire and 2002 House River fire, respectively. Areas salvage logged after the September 2002 field campaign cannot be considered as part of the accuracy assessment.

To investigate the impact of changing minimum mapping unit (MMU) on residual area statistics, residual polygons from the Chisholm and House River Fire were queried into nine minimum mapping unit intervals (0 - 0.01, 0.1 –1, 1.1-5, 5.1-10, 10.1-20, 20.1-40, 40.1-60, 60.1-80, > 80 ha). These intervals were based on previously published data on post-fire residual retention harvesting practices (Lee *et al.*, 2002). To analyze similarities and differences in each study area, we calculate patch metrics including the area of each individual class (CA), the number of patches (NumP) and the mean patch size (MPS) (McGarigal & Marks, 1994). We also calculate the area weighted mean shape index (AWMSI), which provides an indication of the complexity of the patch shapes.

2.3 RESULTS & DISCUSSION

2.3.1 Spectral Separability & Accuracy Assessment

As a forest ages the structure, composition, and spatial patterns of forest cover change (Larson, 1980). Within the boreal ecosystem, tree species maintain their own natural spatial, temporal variability and tree species tend to vary in canopy density, crown closure, forming mixed forest stands that do not always conform to clearly identifiable boundaries. Therefore, it is necessary to capture accurate training areas that consider the different spectral responses between live residuals areas and other land cover types in the image. For the 2002 House River fire, each of the selected training areas were chosen based on their ability to represent the cover types of interest and form unique locations in spectral space. Wetland areas identified during the field campaign formed three separate training areas that did not overlap with the fire-affected or the green residual training areas. For the 2001 Chisholm fire, the separability of the classes was clear for the anthropogenic classes (planning units) and wetland classes. However, some confusion existed between residual forest areas in the northern portion of the Chisholm fire study area, which was affected by a previous fire in 1998 that burnt over many of the forest harvesting cutblocks. These areas now contained trees in various stages of regeneration (Figure 2.6). There was no confusion between regenerating forest and residual patches within the Crow Lake Ecological Reserve, as forest harvesting operations are not conducted in this region due to its conservation status. The classification accuracy of the residual forest areas was assessed using the field verification data. For the 2001 Chisholm

fire, 57 out of 65 validation areas were correctly classified as residual forest for a class accuracy of 88 %. In the House River fire, 92 out of 98 residual forest validation areas were correctly classified to produce a residual forest classification map with 94 % accuracy.

2.3.2 Residual Patch & Shape Level Metrics

The Chisholm and House River study areas are two areas undergoing different land use and land cover change dynamics and the residuals have been detected using two different satellite image sensors. The Chisholm fire was examined with the Landsat ETM+ imaging sensor with a spatial resolution of 28.5 meters and the House River fire with a 4-meter spatial resolution IKONOS image. Residual forest within the fires, residual area is calculated as 33 % of the Chisholm fire and 27 % of the House River fire. Residual forest is also examined according to the nine minimum mapping unit classes between study areas to allow for comparisons of the amount of residual forest within each of the minimum mapping unit classes. Table 1 displays the results of the patch and shape level metrics for the 2001 Chisholm and 2002 House River fires, respectively. In both the Chisholm and House River fire, most of the residual forest area is found within the largest minimum mapping unit class (> 80 ha MMU) (Figure 2.7).

To investigate why the lower MMU classes contain more residual forest in the 2002 House River fire, it is useful to examine the number of residual patches and mean patch size. Analysis of the House River fire residual polygons shows that this fire contains a large number of small area residual patches. The number of patches in the House river

fire at the [< 0.1 ha] class size is 18,844 patches, while the largest MMU class [> 80 ha] contains only 4 residual patches (Figure 2.8). The trend toward smaller number of patches at higher MMU classes is also characteristic of the Chisholm Fire data, where the number of patches decreases from 6,771 in the lowest MMU class [< 0.1 ha] to only 51 patches at the highest MMU class [> 80 ha] (Table 2.2). For the 2002 House River fire, only the largest MMU class [> 80 ha] shows a significant increase in mean patch size that is explained by the large amount of residual forest contained within this class.

From an image classification point of view, the optimal spatial resolution is defined as the point where object size meets sensor spatial resolution (Woodcock & Strahler, 1987; Marceau & Hay, 1999). As the spatial resolution increases so too does our ability to infer smaller area residual patches using conventional pure-pixel based image classification techniques. Therefore, if a satellite image is used to detect residuals, but many of the residuals tend to occur as small or irregular shaped patches, the results may vary significantly if an area is imaged using a different satellite image sensor (Figure 2.9). For example, in conventional pure-pixel mapping approaches to image classification, if we use one type of imagery (i.e. Landsat TM imagery) to detect forest residuals, the sensor capabilities and classification method determine all the potential residual patches we can detect, while implicitly excluding those smaller area sub-pixel patches. Therefore, when examining an area with imaging sensors at differing spatial resolution, the coarser spatial resolution may consider a forested area as a large patch, while at a higher spatial resolution, gaps in the forest canopy can appear. For example, the House River contains 18, 844 patches at the [< 0.1 ha] class size and only 4 patches at the [> 80 ha] class

(Table 2.1). The House River fire captures more smaller area residual patches at the < 0.1 ha MMU class as this area is being observed using the 4-metre spatial resolution IKONOS sensor. With a coarser imaging system such as Landsat ETM+, it is possible that many of these individual residual forest patches would be classified as a single congruent patch. The result is that coarser resolution sensors can lead to lower estimates of the number of patches, but also increase the amount of residual forest occurring within the larger sized MMU classes. The physical size of the study area is also a significant factor and the House River fire study area is a smaller sized area than the Chisholm fire perimeter that needs to be considered when evaluating results across study areas.

When attempting to make comparisons of the number of residual patches and complexity of the shapes of those patches using landscape metrics across different study areas, the choice of observation tool (i.e satellite sensor) and the selection of minimum mapping unit can affect interpretations. The selection of a minimum mapping unit will influence the total number and area of residual forest islands within a fire perimeter (Tables 1 & 2). If a MMU of five hectares is used, patches that are too small for the minimum mapping unit are not considered in the analysis. In previous post-fire residual studies using aerial photography, Eberhart and Woodard (1987) explicitly defined residual forest patches as unburnt patches at least 1ha in size, while Delong and Kessler (2000) defined a residual as an older forest patch ≤10 ha in size based on field data. Such variations in the scale or MMU used for analysis can complicate the process of making comparisons between study areas. Depending on whether residual forest has been

classified using high or low-resolution imagery, a 10 ha MMU can provide very different results in terms of patch size and number of patches within a fire perimeter.

Residual forest areas maintain very different natural shapes/variations in the study area that can affect the calculation of patch and shape level metrics. There are residuals that form large identifiable homogenous stands that have been surrounded by a larger fire affected area. These stands do not occur along the road, but form isolated patches within the fire-affected area. Isolated residuals patches also tend to be found at the perimeter of a linear anthropogenic feature such as a road or transmission line. Finally, there are residuals that do not seem to occur within a larger patch but tend to be found in a region that was not prone to burning such as a wetland (Figure 2.10). To investigate the complexity of the residual shapes in each fire, the areal weighted mean shape index (AWMSI) is calculated. AWMSI is a robust method used to measure the average patch shape or the average perimeter to area ratio for the residuals. AWMSI can highlight those patches that tend to from circular shapes or follow jagged patterns with rough edges (Saura, 2002). This information is important, considering that fire-affected areas do not always have clear transitions between deciduous and coniferous forest stands, or these stands can be modified by the presence and locations of linear features (i.e roads). The AWMSI shows opposite results in each of the study areas. In the House River fire, there are increasing complex patches at lower MMU classes, and a decrease in complexity at the higher MMU classes (Figure 2.11). In certain areas of the fire perimeters, isolated stands maintain bona-fide boundaries between fire affected and residual areas, while in other regions there is a gradual transition from residuals to fire affected areas. Although

forest ecologists can relate residual dynamics to fire and successional processes, such configurations may also be related to fire suppression techniques, via the creation of linear feature firebreaks that were used to extinguish the fire. Therefore analysis of a measure of residual shape complexity (i.e. AWMSI) should be considered relative to any linear feature fragmentation of forest patches by roads, transmission and seismic lines that also found occur within the fire perimeter (Figure 2.12).

Residual locations and shapes are affected by the various LUCC dynamics occurring in an area, making it difficult to compare results from studies using different minimum mapping units. Presently data collected on post fire residuals using interpretations from aerial photography are used to devise forest-harvesting guidelines based on emulating natural disturbances (Lee *et al.*, 2002). However, considering that much of the available data on residuals is based on observations at defined minimum mapping units, it is likely that certain size residual islands are not being included in the analysis of post fire environments. This includes understanding that residual patch sizes and locations can vary in areas undergoing different natural ecological processes, fire histories and LUCC dynamics. Forest management strategies that are based on examining residual data from fire-affected areas should be aware of how anthropogenic features in the landscape and the choice of MMU used can affect residual patch metrics.

The mapping of fire-affected areas has been noted as a research area in need of improvement (Conard *et al.*, 2001). In areas continually affected by extensive linear disturbances, such as the northern Alberta boreal forest, it will become increasingly

difficult to determine how the location, distribution and pattern of residuals will change in landscapes over time. For example, areas such as the Chisholm Fire study area that are undergoing increasing linear feature expansion, may show a greater number of residual patches than areas that are not affected by the same degree of linear disturbance. Local weather conditions, the timing of year and image acquisition date, as well as the choice of satellite image and minimum mapping unit and influence of linear features can affect results and interpretations. Therefore, an initial step towards developing meaningful characterizations of post-fire land cover will include developing residual classification schemes that will allow for increasingly flexible integration of information collected from various imaging sensors. Thorough investigations of the number and size of residual forest patches in fire affected areas will also require carrying out post-fire residual studies not only in the province of Alberta, but also in other jurisdictions and countries that are not undergoing the same forest harvesting practices or expansion of linear features that are occurring in the province of Alberta.

2.4 CONCLUSIONS

Land cover classifications, in areas affected by forest fire, need to move beyond descriptive and qualitative definitions (i.e. burnt area) and provide meaningful information on the features occurring within disturbed areas. The goal of this chapter was to examine the use of high and medium resolution imagery for residual detection and to analyze the distributions of residuals within fire-affected areas. This study demonstrates that medium and high-resolution satellite imagery can be used to detect and examine post-fire residuals that occur within fire perimeters with > 88 % classification accuracy.

A hybrid unsupervised masking and supervised image classification techniques were able to isolate the residual areas from non-target cover types within the image scene Patch metrics derived from classified residuals highlight that the largest minimum mapping unit (MMU) classes contain the least number of residual patches, but the highest amount of residual forest. The spatial resolution of the imaging sensor used and the size of the minimum mapping unit (MMU) used for analysis affect residual patch and shape metrics. At a coarse resolution, residual forest can be classified as large area patches, while if the same area was observed at high resolution smaller area patches can be identified, thereby increasing estimates of the number of patches in a fire perimeter. Linear features disturbances within the landscape dissect residual patches in the landscape, affecting the derivations of residual patch and shape metrics, complicating direct comparisons of residual patch size and numbers between study areas. The results of this study serve as an important guideline for the use of data derived from remote sensing platforms into residual retention forest harvesting protocols that aim to base forest harvesting practices on emulating fire in the landscape.

2.5 LITERATURE CITED

Amiro, B. D., Stocks, B.J., Alexander, M.E., Flannigan, M.D., Wotton, B.M. 2001. Fire, climate change, carbon and fuel management in the Canadian boreal forest. *International Journal of Wildland Fire,* 10, 405-413.

Amiro, B.D. & Chen, J.M. 2003. Forest fire scar aging using spot-vegetation for Canadian ecoregions. *Canadian Journal of Forest Resources*, 33, 1116-1125.

Bonan, G.H. & Shugart, H.H. 1989. Environmental Factors and Ecological Processes in Boreal Forests. *Annual Review of Ecology and Systematics*, 20, 1-28.

Bougeau-Chavez, L.L. Kasischke, E.S., Brunzell, S., Mudd, J.P. & Tukman, M. 2002. Mapping fire scars in global boreal forest using imaging radar data. *International Journal of Remote Sensing*, 23 (20), 4211-4234.

Chisholm Fire Review Committee Final Report. Alberta Sustainable Resource Development: October 2001 53pp)[http://www3.gov.ab.ca/srd/forests/chisholm/].

Conard, S. G., Hartzell, T., Hillbruner, M.W. & Zimmerman, G.T. 2001. Changing fuel management strategies-- The challenge of meeting new information and analysis needs. *International Journal of Wildland Fire,* 10, 267-275.

Congalton, R.G. 1991. A Review of Assessing the Accuracy of Classifications of Remotely Sensed Data. *Remote Sensing of Environment*, 7, 35-46.

Delong, S., Kessler, W. 2000. Ecological characteristics of mature forest remnants left by wildfire. *Forest Ecology and Management*, 131, 93-106.

Diaz-Delgado, R., Lloret, F. & Pons, X. 2003. Influence of fire severity on plant regeneration by means of remote sensing imagery. *International Journal of Remote Sensing*, 24 (8), 1751-1763

Dorling, D. 1998. Human Cartography: when it is good to map? *Environment and Planning A*, 30, 277-288.

Eberhart, K.E. & Woodard, P.M. 1987. Distribution of residual vegetation associated with large fires in Alberta. *Canadian Journal of Forest Resources*, 17, 1207-1212.

Garcia–Haro, F., Gilabert, M.A., Melia, J. 2001. Monitoring fire-affected areas using Thematic Mapper data. *International Journal of Remote Sensing*, 22 (4), 533-549.

Greene, D.F., Zasada, J.C., Sirois, L., Kneeshaw, D., Morin, H., Charron, I. & Simard, M. 1999. A review of the regeneration dynamics of North American boreal forest tree species. *Canadian Journal of Forest Resources*, 29, 824-839.

Harley, J.B. 1989. Deconstructing the map. *Cartographica*, 26 (2), 1-20.

Keane, R. E., Burgan, R. & van Wagtendonk, J. 2001. Mapping wildland fuels for fire management across multiple scales: Integrating remote sensing, GIS, and biophysical modelling. *International Journal of Wildland Fire*, 10, 301-319.

Kuhry, P. 1994. The role of fire in the development of Sphagnum-dominated peatlands in western boreal. *Journal of Ecology*, 82 (4), 899-910.

Larson, J.A. 1980. The Boreal Ecosystem. New York. Academic Press (500 pp).

Lee, P., Smyth, C., & Boutin, S. 2002. Large-scale planning of live treed residuals based on a natural disturbance-succession template for landscapes. Alberta Research Council, Vegreville.

Marceau, D. J. & Hay, G.J. 1999. Remote sensing contributions to the scale issue. *Canadian Journal of Remote Sensing*, 25 (4), 357-366.

Martell, D. 2001. Forest Fire Management. In Johnson, E. & Miyanishi, K. 2001. Forest Fires: Behaviour and Ecological Effects. Academic Press (594 pp).

McGarigal, K. & Marks, B. 1994. FRAGSTATS*ARC: Spatial pattern analysis program for quantifying landscape structure (Version 2.0). Corvallis, OR.

Miller, J. & Yool, S. 2002. Mapping forest post-fire canopy consumption in several overstory types using Landsat TM and ETM+ data. *Remote Sensing of Environment*, 82, 481-496.

Pereira, M.C, & Setzer, A.W. 1993. Spectral characteristics of fire scars in Landsat 5 TM images of Amazonia. *International Journal of Remote Sensing,* 14 (11), 2061-2078.

Riaño, D., Chuvieco, E., Ustin, S., Zomer, R., Dennison, P., Roberts, D. & Salas, J. 2002. Assessment of vegetation regeneration after fire through multitemporal analysis of AVIRIS images in the Santa Monica Mountains. *Remote Sensing of Environment,* 79, 60-71.

Richards, J.A. 1994. Remote sensing digital image analysis. Berlin: Springer-Verlag (281pp).

Rogan, J., & Yool, S.R. 2001. Mapping fire-induced vegetation depletion in the Peloncillo Mountains, Arizona and New Mexico. *International Journal of Remote Sensing*, 22 (16), 3101-3121.

Rowe, J. & Scotter, G. 1973. Fire in the Boreal Forest. *Quaternary Research*, 3, 444-464.

Sánchez-Azofeifa, G. A., Kachmar, M., Kalácska, M. & Hamilton, S. 2003. Experiences in Field Data Collection for Land Use and Land Cover Change Classification in Boreal and Tropical Environments. In Methods for Remote Sensing of Forests: Concepts and Case Studies. Kluwer Academic Publishing (pp.433 – 446).

Sandberg, D.V., Ottmar, R.D., Cushon, G.H. 2001. Characterizing fuels in the 21st century. *International Journal of Wildland Fire*, 10, 381-387.

Saura, S. 2002. Effects of minimum mapping unit on land cover data spatial configuration and composition. *International Journal of Remote Sensing*, 23 (22), 4853-4880.

Schieck, J. & Hobson, K.A. 2000. Bird communities associated with live residual tree patches within cut blocks and burned habitat in mixedwood boreal forests. *Can. J. For. Res.*, 30, 1281-1295.

Song, C., Woodcock, C., Seto, K., Lenney, M. & Macomber, S. Classification and change detection using Landsat TM data: When and how to correct atmospheric effects? *Remote Sensing of Environment*, 75, 230-244.

Sousa, W.P 1984. The Role of Disturbance in Natural Communities. *Annual Review of Ecology and Systematics,* 15, 353-391.

Stehman, S.V & Czaplewski, R.L. 1998. Design and Analysis for Thematic Map Accuracy Assessment: Fundamental Principles. *Remote Sensing of Environment*, 64, 331-344.

Strand, G.H., Dramstad, W., & Engan, G. 2002. The effect of field experience on the accuracy of identifying land cover types in aerial photographs. *International Journal of Applied Earth Observation and Geoinformation*, 4, 137-146.

Strong, W.L. & K.R., Leggat. 1992. Ecoregions of Alberta. Alberta Forestry, Lands & Wildlife. Edmonton, Alberta.

Sunar, F., Özkan, C. 2001. Forest fire analysis with remote sensing data. *International Journal of Remote Sensing*, 22 (12), 2265-2277.

Tou, J.T. & Gonzalez, R.C. 1974. Pattern Recognition Principles. Addison-Wesley Publishing Company (377pp).

White, J.D., Ryan, K.C., Key, C.C., & Running, S.W. 1996. Remote Sensing of Forest Fire Severity and Vegetation Recovery. *International Journal of Wildland Fire*, 6 (3), 125-136.

Woodcock, C.E. & Strahler, A.H. 1987. The Factor of Scale in Remote Sensing. *Remote Sensing of Environment,* 21, 311-322.

Zukowskyj, P.M., Bussell, M.A., Power, C., & Teeuw, R.W. 2001. Quantitative accuracy assessment of contextually filtered classified images. *International Journal of Remote Sensing*, 22 (16), 3203-3222.

Table 2.1. Residual forest patch metrics as a function of minimum mapping unit for the 2002 House River Fire derived from a supervised maximum likelihood classification on a 4-m resolution IKONOS image.

Metrics	<0.1	0.11–1	1.1-5	5.1-10	10.1-20	20.1-40	40.1-60	60.1-80	>80
Class Area (ha)	190.8	263.6	218.8	74.2	50.9	155.5	155.7	61.0	1643.9
Number Patches	18844.0	835.0	103.0	11.0	4.0	5.0	3.0	1.0	4.0
Mean Patch Size (ha)	3.3	149.2	212.6	74.2	50.9	155.5	155.7	61.0	1643.9
AWMSI	131.0	1079.8	469.1	82.4	32.5	61.3	34.5	9.5	75.6

Table 2.2. Residual forest patch metrics as a function of minimum mapping unit for the 2001 Chisholm Fire derived from a supervised maximum likelihood classification on a 28.5-m resolution Landsat ETM+ image.

Metrics	<0.1	0.11–1	1.1-5	5.1-10	10.1-20	20.1-40	40.1-60	60.1-80	>80
Class Area (ha)	423.2	1887.9	2790.5	1594.0	1669.8	1828.4	840.7	679.3	26116.9
Number Patches	6771.0	5278.0	1244.0	224.0	117.0	66.0	17.0	10.0	51.0
Mean Patch Size (ha)	0.2	8.4	192.9	528.5	1144.4	1618.1	840.7	679.3	26116.9
AWMSI	3.4	22.8	133.6	192.3	255.5	232.7	90.8	55.4	511.9

Areal Weighted Mean Shape Index (AWMSI)

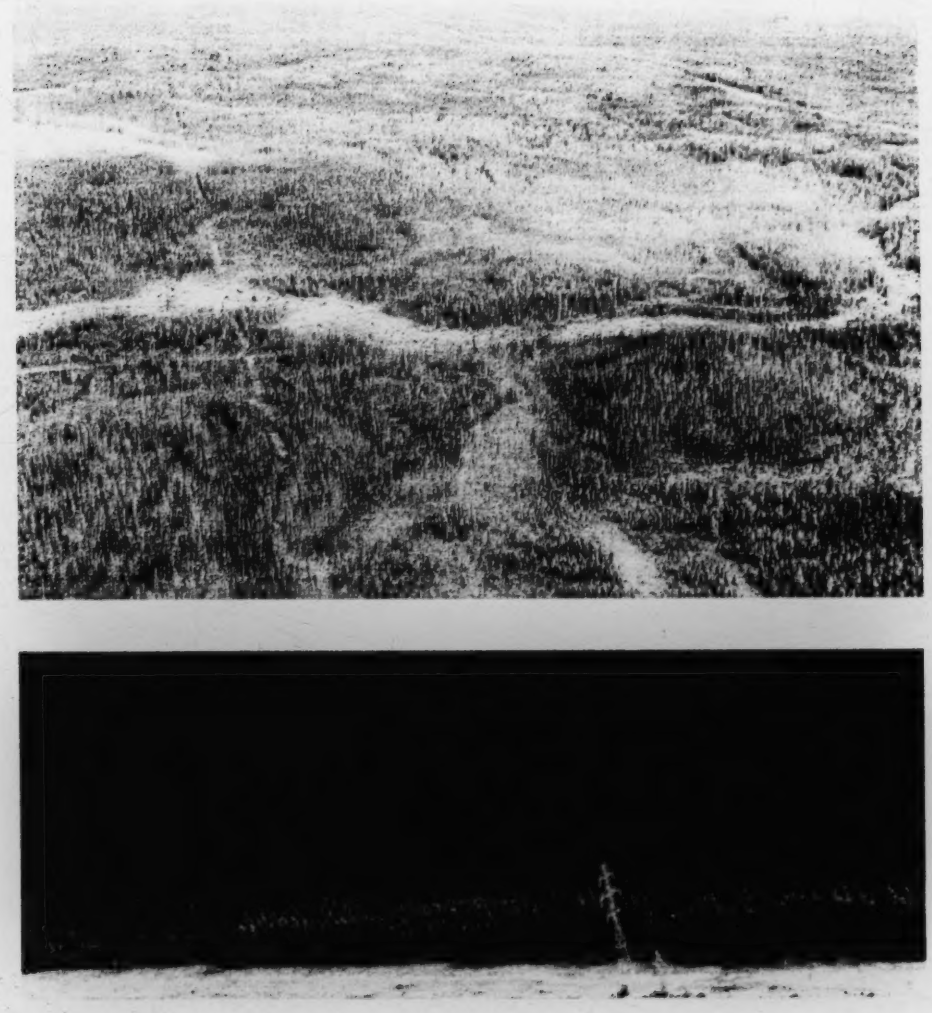

Figure 2.1 Oblique view of the locations and geometric shapes of residual patches that occur a) within fire perimeters; and b) along transmission lines.

Figure 2.2. Location of the Crow Lake Ecological Reserve (affected by the 2002 House River fire) and the 2001 Chisholm Fire, overlaid onto the border of the Province of Alberta, Canada.

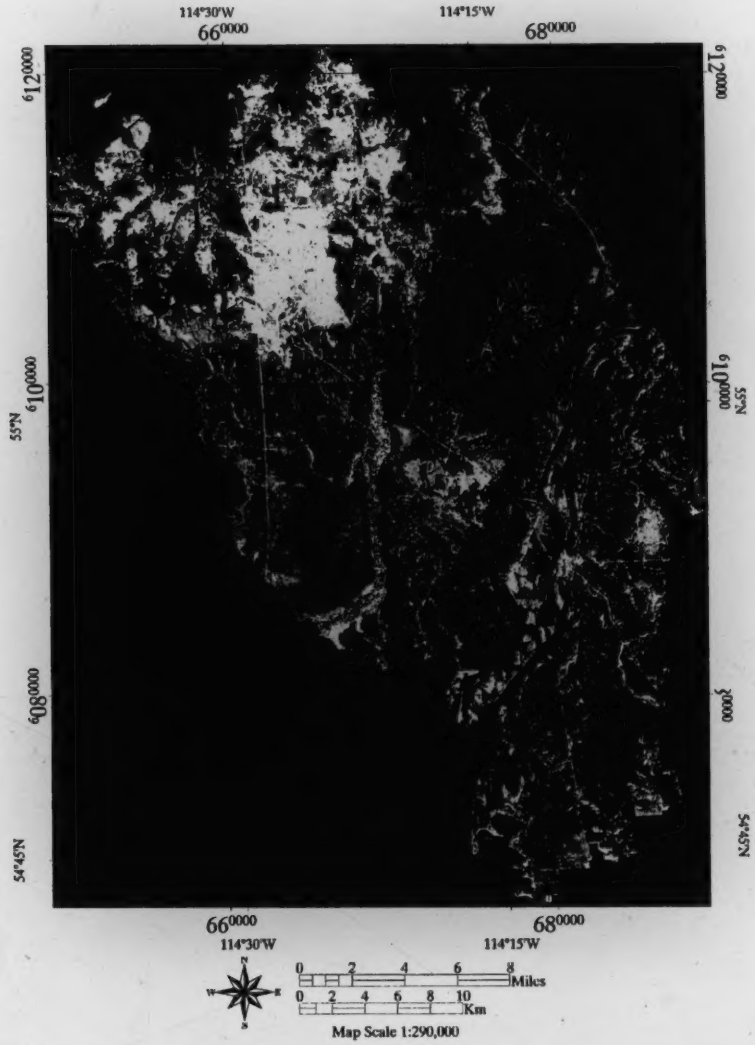

Figure 2.3 Outline of the 2001 Chisholm Fire perimeter represented by a 3-band image composite (bands 5 4 3) of the Landsat ETM+ image. Darker colors represent those areas burnt in the fire. Green colored areas represent live vegetation cover. The Landsat ETM+ image was subset from the original full image scene (Path 43 Row 22) and georectified using a image to vector registration by selecting ground control points at key road intersection using 1: 20, 000 vector access data. The image was reprojected to Universal Transverse Mercator (UTM) Zone 11, NAD 83 for subsequent processing.

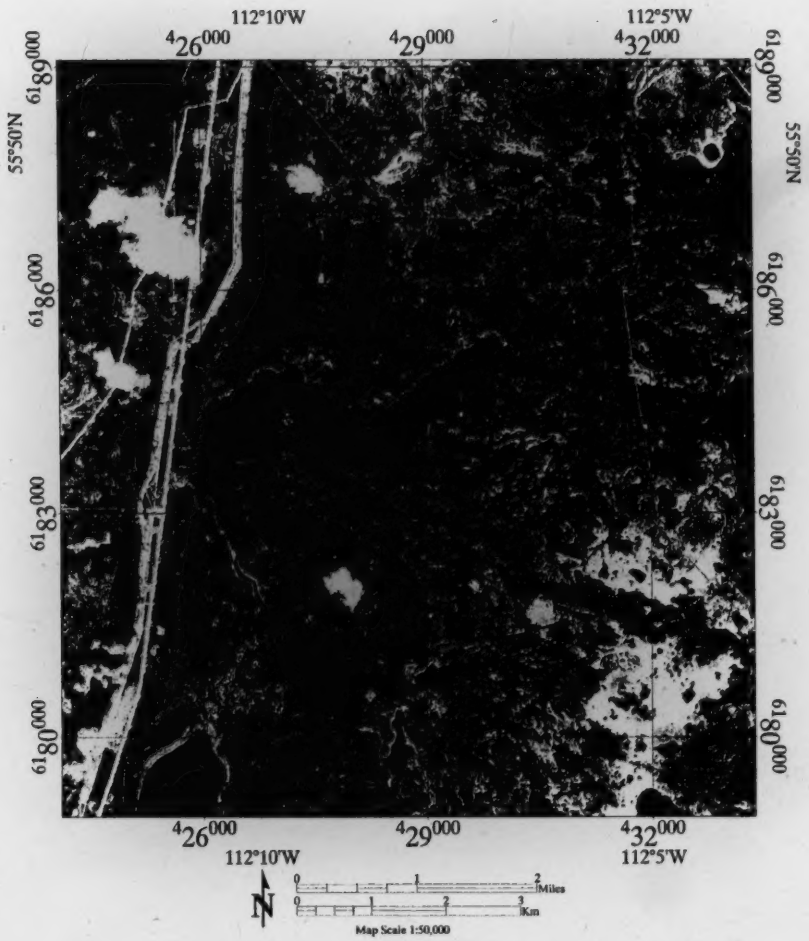

Figure 2.4 3-Band Image Composite (Bands 4 3 2) of the IKONOS image that was acquired over the House River fire on August 29, 2002. Red colored areas represent residual forest, while green color regions represent areas burnt by the fire. Crow Lake is located near the centre of the image. For the 2002 House Rive Fire, an IKONOS multispectral image was acquired over a 10 x 10 km area (Crow Lake Ecological Reserve). This image was reprojected to UTM Zone 12 and the boundary of the IKONOS scene formed the study area.

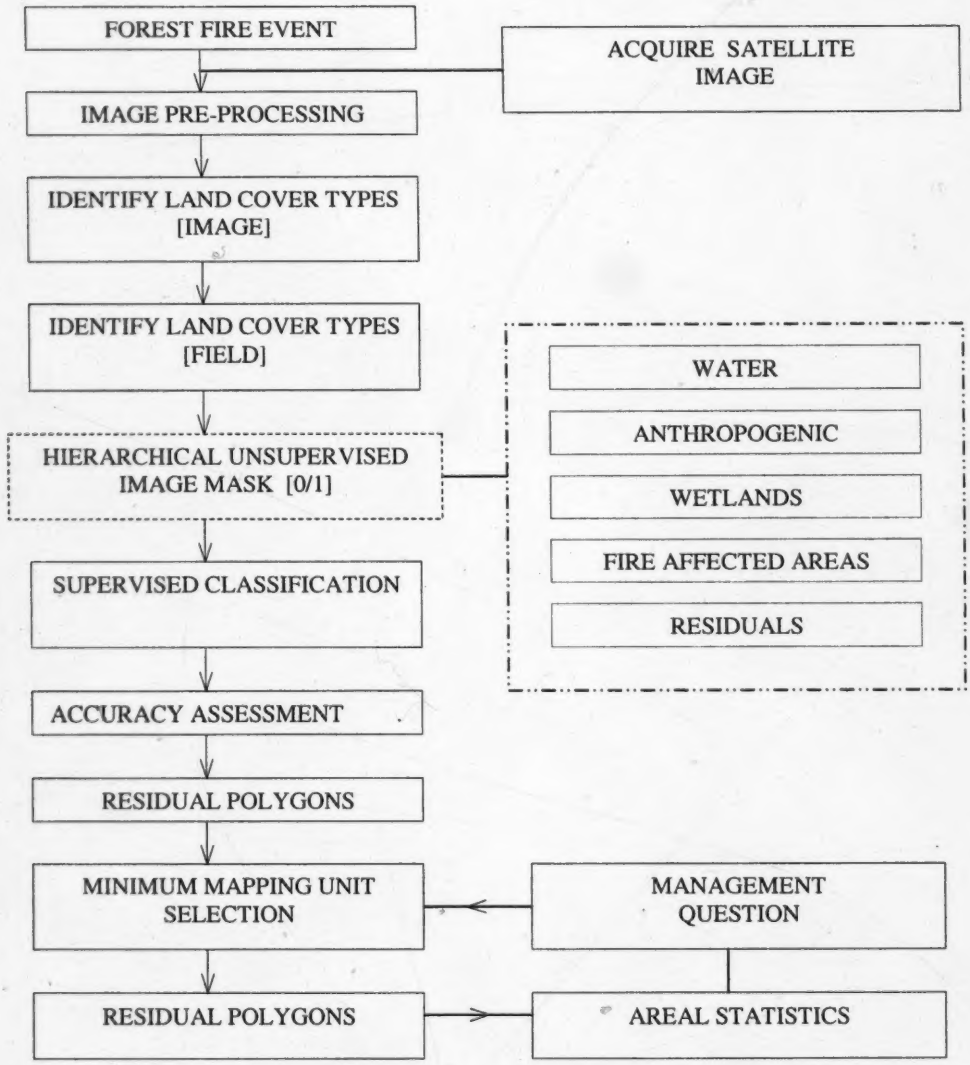

Figure 2.5 Flowchart outlining the methodological processes involved in detecting and analyzing residual forest cover using Landsat ETM+ and IKONOS imagery.

Figure 2.6 3-Dimensional visualization of training sites within the a) 2001 Chisholm and b) 2002 House River fires.

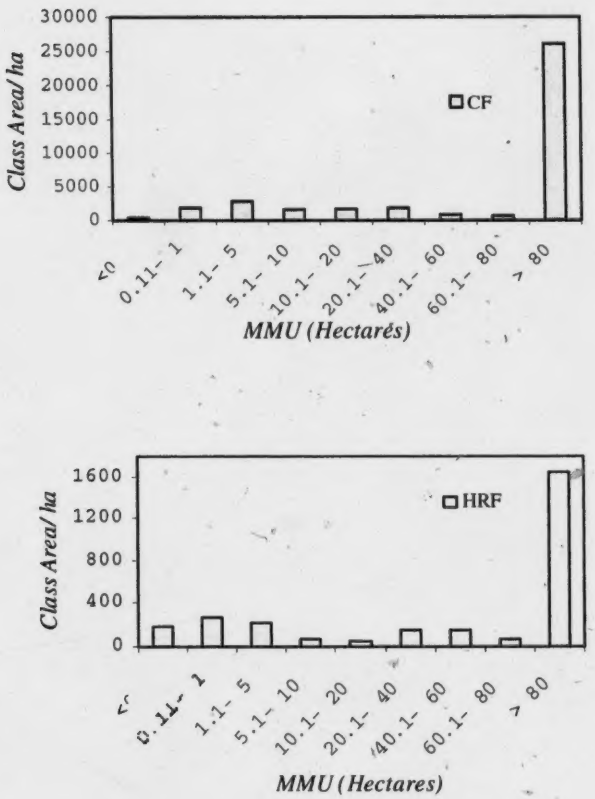

Figure 2.7 Total area of the residual forest classes calculated as a function of minimum mapping unit from a classified Landsat ETM+ image acquired over the perimeter of the 2001 Chisholm fire and from a classified IKONOS image acquired over the 2002 House River Fire.

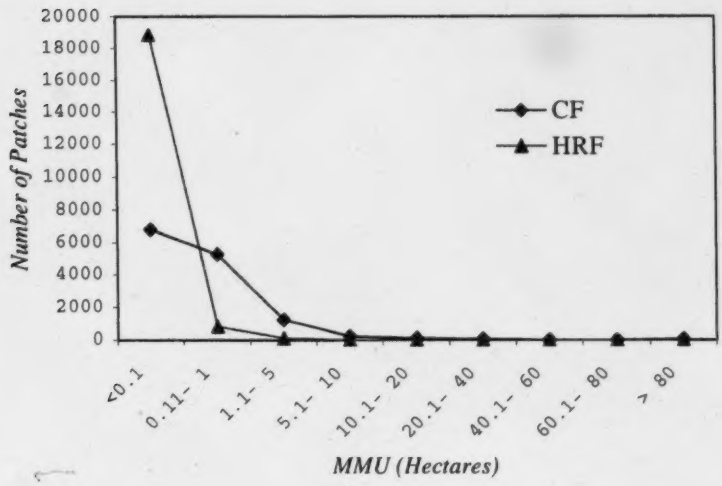

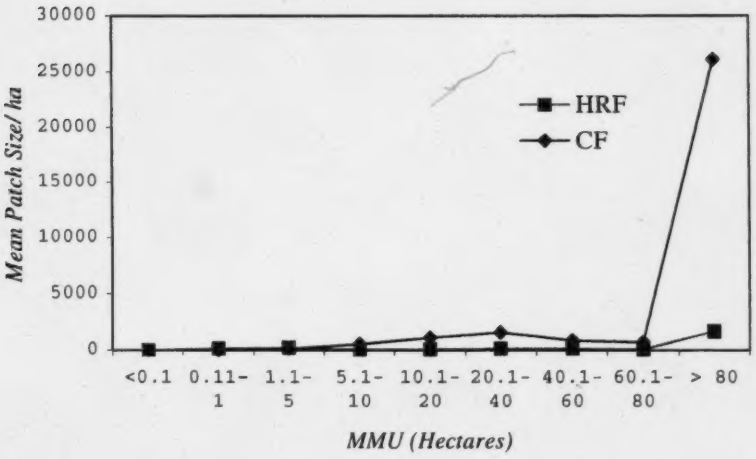

Figure 2.8 Number of Patches and Mean Patch Size calculated as a function of minimum mapping unit for the perimeter of the 2001 Chisholm and 2002 House River Fires.

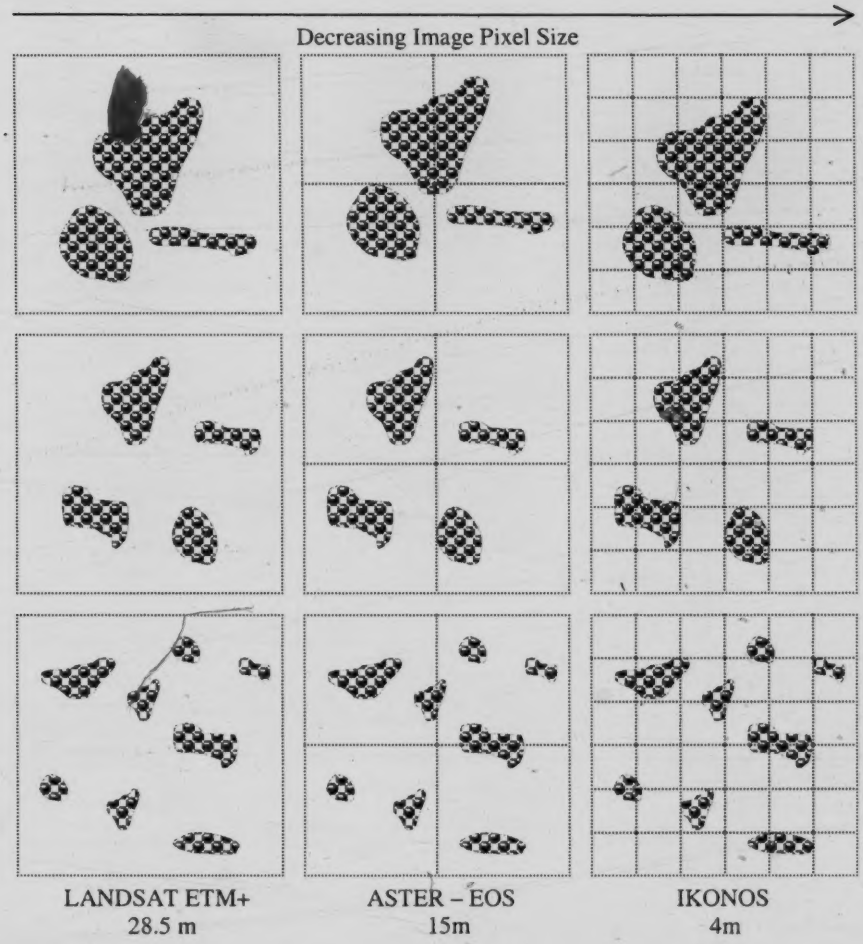

Figure 2.9 Bird's eye view of the effect of increasing sensor spatial resolution on different sized residual forest patches overlaid onto a grid representing sensor field of view at arbitrary 28.5, 15 and 4 - metre sensor spatial resolution.

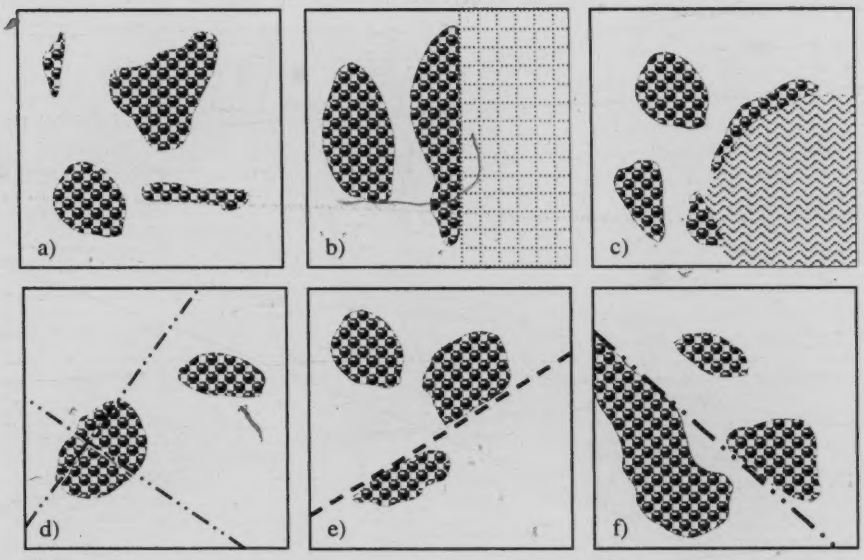

Figure 2.10 Bird's-eye-view pictorial representation of the locations and geometric shapes of unburnt [residual] forest patches located within the Chisholm (2001) and House River (2002) fire perimeter occurring as a) isolated forest islands; b) between agricultural fields; c) bordering lakes; d) along seismic lines; e) along road edges; and f) along transmission lines.

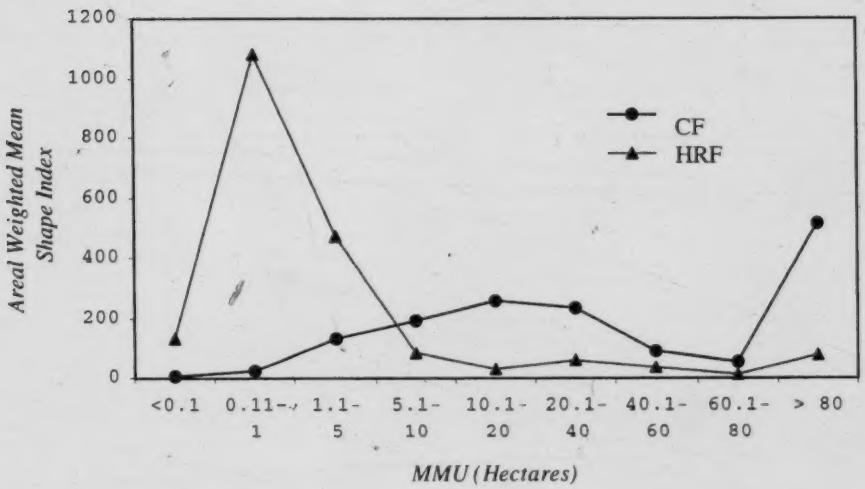

Figure 2.11 Areal weighted mean shape index calculated as a function of minimum mapping unit for the perimeter of the 2001 Chisholm and 2002 House River fires.

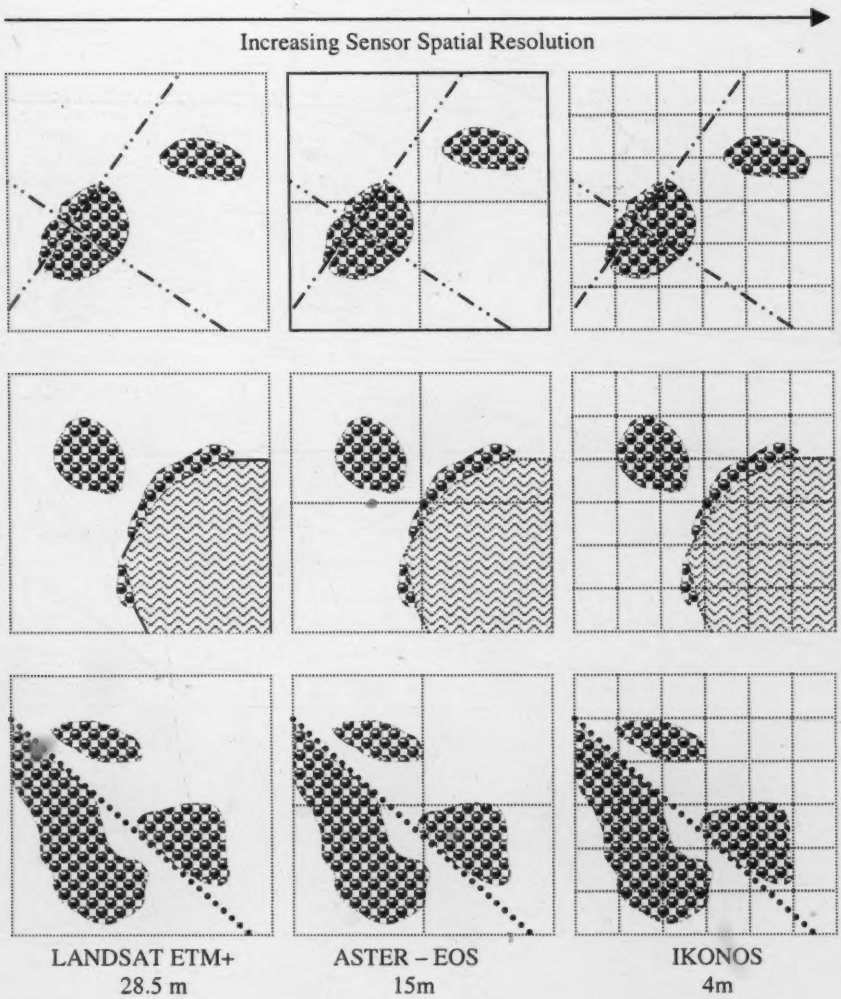

Figure 2.12 Pictorial representation of the effect of increasing sensor spatial resolution on different sized residual forest patches affected by a) seismic lines; b) bordering lakes; and c) roads overlaid onto a grid representing sensor field of view at 28.5, 15 and 4 - metre sensor spatial resolution perimeter.

CHAPTER 3

FOREST COVER CLASSIFICATION IN INDUSTRIALIZED MOUNTAIN TERRAIN USING LANDSAT TM 5 IMAGERY

3.1 INTRODUCTION

Land use and cover change (LUCC) and its associated impacts on global environmental and climate change are a growing concern for the international scientific community (Dale, 1997; Lambin *et al.*, 2001). Areas particularly prone to LUCC are mountain environments because of increasing industrial (i.e. forest harvesting) and recreational (i.e. ski resorts) activities in these areas (Jansky *et al.*, 2002). Increasing LUCC highlights the need for forest protection and conservation in mountain environments (Becker & Bugmann, 2001), which are estimated to contain one fourth of the world's forest resources (Gruen & Murai, 2002). Monitoring such areas can be difficult, though, as accurate information on the status of forest cover in such regions is often either non-existent or unreliable (Matsushita & Masayuki, 2002; Welch *et al.*, 2002).

Spaceborne remote sensing can take snapshot images of land cover over large inaccessible areas on the earth's surface, making it increasingly useful for long-term land and forest cover monitoring (Masek *et al.*, 2001). However, mountain areas pose unique challenges for forest cover classification as accurate *in situ* ground truthing data may be difficult to collect and topographic shading is problematic in high relief

areas. Therefore, instead of using ground data to aid image classification, ancillary data sources (i.e. aerial photography) are commonly used. The drawback in utilizing aerial photography is that it does not allow for the flexibility of collecting detailed information on the various forest cover types nor can it provide insight into local land use practices taking place in a given region (Sánchez-Azofeifa *et al.*, 2003). Aerial photography may also lack sufficient spatial coverage and may not have been acquired at a similar time of year as the satellite imagery. Nevertheless, due to the associated costs of field campaigns in support ground data collection for image classification, aerial photography often serves as a surrogate data source for ground data verification.

The second challenge to forest cover classification in high relief areas relates to the effect of topographic shading. Topographic shading is caused when the geometry between the sun, target and the imaging sensor (Proy *et al.*, 1989) varies as a function of local topography thus modifying the illumination received by a given surface type. Topographic correction of satellite imagery can improve the ability to discriminate between cover types in mountain areas (Richter, 1998). These correction methods have been further refined by incorporating digital elevation models that enhance the modelling of variation in local mountain slope and aspect (Fahsi, 2002). However, both the coarseness of the digital elevation models used in the topographic correction process and the ruggedness of the mountain terrain are still limiting factors in topographic correction.

Recreational and industrial practices occurring in mountain areas can also complicate the ability to classify forest cover using satellite imagery. Forestry thinning and harvesting operations, for example, can modify the structure (i.e. density), composition (i.e. age, # of species & # of trees) and spatial patterns of forest cover types. Forest harvesting disturbances may not necessarily involve an actual land cover transformation, but both the location and severity of the disturbance can contribute to increased landscape heterogeneity (Sousa, 1984). Physical land cover transformations can also occur when one forest cover type is harvested from an area and then the same area is replanted with another tree species. In such environments, the impacts of land use and cover change can lead to both immediate and long-term modifications to the natural ecotones that exist between forest communities.

Changes to the openness, age and density of forest cover types in mountain areas that result from such LUCC dynamics across multiple slope gradients and elevations, can lead to increased intra-class variability in the spectral reflectance of a single forest cover. These changes can also reduce the inter-class variability between forest cover types. The cumulative impact of long term LUCC in an area can lead to the formation of "industrialized landscapes", which may be defined by prolonged LUCC processes that alter the spectral reflectance properties of the pre-existing land and forest cover to a new state. Such landscapes are problematic for supervised image classification techniques that require the selection of *a priori* training areas to classify similar land cover types within an image scene. Increased intra class variability has

been noted as a cause of misclassification of high-resolution imagery using conventional supervised image classification techniques (Hsieh *et al.*, 2001).

Satellite image based classifications of forest cover in mountain environments typically focus on correcting images for topographic shading before proceeding to classify the forest cover types. This research differs in its approach to forest cover classification using satellite imagery, as spectral separability is computed for each of the forest cover classes using Jeffries-Matusita (JM) distance. The JM separability is then related to anthropogenic processes occurring on the highly industrialized mountain region. Forest cover types are then classified using the spectral angle mapper using training areas selected from the Landsat TM imagery (28.5-m resolution) on Mt. Naeba, in the central part of Honshu, Japan.

3.2 STUDY AREA

3.2.1. Study Area & Forest Cover Classes

The Mt. Naeba study area is located on the southern part of the Niigata Prefecture at the boundary between Nagano and Niigata Prefecture in the central part of Honshu, Japan (36 ° 51′ N and 138 ° 41′ E) (Figure 3.1). In the study area, Beech forest (*Fagus crenata)* dominates the northern slope of the Naeba Mountains over a range of altitudes between 550 m and 1,550 m (Kira, 1949). Species of beech, birch, mixed deciduous forest and cedar are also located within this study area. In the 1940's,

beech forest dominated the study area (Kakubari, 1991), but the forest community has since changed through both forest harvesting activities and the creation of a winter ski resort. In addition, ongoing forest harvesting practices have created uneven aged beech, cedar, and birch forest stands throughout the region. Typically, younger stands of birch (*Betula ermanii*) are located above 1350 m, after clear cutting since ca. 1953, while older birch stands are found at higher elevations (1650m). Although Japanese cedar (*Chriptomeria japonica*) is found within the study site, it is not an endemic species but a product of replanting initiatives. Cedar tends to be located in the lowland areas at the base of the mountains (less than 1000 metres) and from there creeps upward along the based of the mountain slopes. A mixed deciduous forest cover class also exists that consists mainly of Beech *Fagus Crenata*, Oak *Quercus mongolica*, and Bamboo *Sasa krylensis*. This forest class also comprises less dominant species such as *Magnolia obovata Betula ermanii, Betula maximowicziana, Cornus Controversa, Vibirum furcatum, Acer rufinerve, Acer nipponicum,* and *Acer Japonicum*.

The cumulative impacts of anthropogenic surface disturbances such as roadways, ski hills, chairlifts, gondolas and chalets as well as a network of hydro-electric transmission lines have altered the natural shapes of many of the forest cover types on Mt. Naeba. For example, before construction of the transmission towers, substantial areas of beech forest cover were cleared for the right of way under these lines. Following the installation of the transmission towers, the disturbed areas were colonized by a dense natural bamboo understory that remains today. Further

information on the region can be found in (Yamada & Maruyama, 1962; Maruyama 1971,1977; Kakubari 1977, 1987).

3.3 METHODOLOGY

3.3.1 Image Pre-processing

Figure 3.2 outlines the process of classifying and examining the forest cover types in this area. To remove dark current and path radiance biases, pixels were selected in a deep lake in order to conduct a dark object correction on the original Landsat TM scene (Kruse, 1993). Following this process the Landsat TM 5 scene and digital elevation model (DEM) were subset to the outline of the Mt. Naeba study area. Slope and aspect layers generated from the DEM were used as inputs for the cosine corrected topographic correction (Feng *et al.*, 2003):

$$NormalizedRadiance = RawRadiance * (\cos\theta / \cos i)$$

where θ is the solar zenith angle at the time of acquisition and i is the local incidence angle, which can be determined using the DEM and the following equation:

$$\cos i = \cos\beta\cos\theta + \sin\beta\sin\theta\cos(\lambda - \phi)$$

where β is the terrain slope (degrees), ϕ is the solar azimuth angle at time of image acquisition and λ is the local terrain aspect. *RawRadiance* represents the LANDSAT TM detected radiance ($(W/m^{-2}\ \mu m^{-1}\ sr^{-1})*100$) after removal of the diffuse light component using the dark object correction. A complete description of this process can be found in Feng *et al.* (2003). The original and topographically corrected images are shown in figure 3.3ab.

3.3.2 Field Data Collection

To capture ground data to support image classification, two field campaigns were conducted at Mt. Naeba in October 2001 and August 2002. In the first campaign, a preliminary classification scheme was developed to represent the dominant forest cover types in the area. This included three deciduous forest cover classes (birch, beech, and mixed deciduous) and one coniferous forest class (cedar). Training sites for the birch, beech, cedar, and mixed deciduous forest types were chosen in vehicle accessible areas within the study area that were clearly visible on the Landsat imagery. Each forest cover training area is assumed to represent a homogeneous representation of the cover type. Training areas were labelled on the map and their locations recorded with a global positioning system (GPS) device. In the second campaign, field data was collected to validate the accuracy of the forest classification following topographic correction. A total of sixty-nine validation areas representing the forest cover types were collected.

3.3.3 Training Area Selection & Spectral Separability

Following the October 2001 field campaign, non-target cover types (water, ski slopes, urban areas) were extracted from the satellite image using an unsupervised [image-masking] approach. To determine the degree of separability for the birch, beech, cedar, and mixed deciduous training sites, spectral separability was computed using the Jeffries-Matusita (JM) distance (Richards, 1994). The Jeffries-Matusita distance was selected to assess the ability of the image classifier to discriminate between the different forest cover types because it accounts for the spectral variability among (intra-class) and between (inter-class) forest cover types. A Jeffries-Matusita value of 2.0 between training areas implies that these two classes are 100% separable. Spectral separability can be useful in developing and refining training areas or choosing viable forest cover types that could be represented in a forest cover classification scheme. Attempts were made to select those training areas that could provide at least a high separability value of (>1.98) (Table 3.1), however not all classes could not achieve this high level of separability. These forest training areas were displayed in *n*-dimensional feature space (Landsat TM bands 345) to assess where and which forest cover types were distinct or overlapped.

3.3.4 Supervised Spectral Angle Mapper [SAM] Classifier

The forest training areas captured during the October 2001 field campaign were used as inputs for the spectral angle mapper classifier [SAM] (Kruse *et al.*, 1993). The SAM uses the *n*-dimensional angle to compare satellite image spectra to the reference (training area) in the Landsat TM 5 image. Rather than using conventional statistical techniques based the Euclidean distance to classify land cover types, SAM was deemed more appropriate for high relief areas because it treats the spectra as vectors in a space with dimensionality equal to the number of bands. The algorithm then compares the angle between the reference spectrum vector and each pixel vector in *n*-dimensional space. This technique emphasizes differences in spectral shape rather then amplitude, the later having dependence on topographic variations. Smaller vector angles between spectra represent closer matches to the training area spectrum and can be grouped into the cluster represented by the reference spectrum (Kruse *et al.*, 1993). A cut off angle of .10 radians was chosen for the deciduous and coniferous cover types. However, the angle was slightly increased to .15 radians for the birch class as this class exhibited greater intra class variability in n-dimensional space than the other forest cover types. The SAM algorithm outputs an image containing the forest classes and the non-target cover types (i.e. anthropogenic classes).

The classified SAM output image was then filtered using a 3x3 median filter to eliminate pixels that are not surrounded by any other pixels of the same class (Zukowskyj *et al.*, 2001). Sixty-nine validation areas that were collected in August

2002 were then used to assess the forest cover classification accuracy (Table 2). Finally, the forest cover classes were converted to vector polygons to be able to analyze the landscape structure of the forest classes. The total landscape area, number of patches and mean patch size of the forest cover classes (McGarigal & Marks, 1994) were computed and are presented in table 3.3.

3.4 RESULTS & DISCUSSION

3.4.1 Forest Cover Spectral Separability

Training areas representing the beech, birch, mixed deciduous and cedar forest were selected in the image to characterize these forest cover types across the study area. The JM distance measure and views of the spectral clusters in *n*-dimensional space can highlight those forest cover types that are becoming confused through increasing intra-class and decreased inter-class reflectance. Both these tools can then be used to improve the ability to determine what forest classes can be more accurately classified in the image scene.

The JM separability values between the forest cover types for the pre and post topographically corrected image are shown in table 3.1.The JM values for the training areas prior to image topographic correction shows that all the deciduous forest cover types have a high degree of separability (JM value > 1.98) with the coniferous cedar forest class. The lowest JM distance values are found between the deciduous forest

cover types. The mixed deciduous and beech classes maintains a low JM value of 1.92 and Beech and Birch forest training areas have the lowest JM values 1.69. Examining these classes in the 2-dimensional viewer shows that the beech and birch forest (JM value 1.69) overlap in the near infrared (band 4) and short wave (band 5) infrared bands (Figure 4ab). Although the beech class does appear to be more tightly grouped along the mean pixel value, there is a lot of internal variation within this class. The birch class pixels form an elongated array along Bands 4 and 5 and appear to form three distinct pixel clumps. The characteristic of these two forest classes contrasts that of the coniferous cedar forest pixels, which tend to form a tighter cylindrical pattern with less internal variability in their spectral cluster.

Following topographic correction, the ability to discriminate between forest cover types in the rugged mountain area varies as a function of forest cover type. JM distance between the deciduous and the coniferous forest cover, for example, showed minimal improvement. This lack of improvement reflects the already high inter-class separability between the deciduous and coniferous cover types (JM > 1.98) even before the topographic correction (Figure 3.4). The ability to discriminate between the previously confused beech and birch did improve following the topographic correction from a JM distance of 1.69 to a higher value of 1.74. This is a marginal improvement in separability however and still considered as a low separability between these two deciduous forest classes. The low separability (JM value 1.69) between the mixed deciduous and beech forest classes before topographic correction, decreased to a JM value of 1.34 following the topographic correction. The decreased

separability between the mixed deciduous and beech forest may indicate that this cover types is not sufficiently distinct from the beech class, particularly if the mixed deciduous forest training areas contain a high proportion of beech trees that is characteristic of this class.

An examination of the forest cover classes in 2-dimensional space following the topographic correction shows that the birch and beech appear to shift closer together along Landsat band 4 and 5. Additionally, the previously noted three independent clusters of birch appear to have been smoothed into a larger group and there are no longer three distinct clusters (Figure 3.4). The beech and mixed deciduous classes show a lower interclass distance, indicating that the brightness variations that result from topographical changes may have been slightly dampened after topographic correction. The cedar forest class underwent little to no change in shape or distance from the birch or beech forest classes.

Human alterations to forest cover types across a study area can affect the spectral reflectance properties of a given forest cover type. These structural and composition changes to the forest may dictate whether or not suitable training areas can be use to represent a forest cover type across the study area. The pre and post-topographic correction training areas were examined in a 3-band spectral space composite to examine if the forest clusters disperse in a distinct trajectory from that caused by topography in the Landsat TM bands (Figure 3.5). Viewing the forest clusters in Landsat bands 347 before the topographic correction shows the spread out beech

forest classes and more distinctly shows the three distinct clusters of birch forest. Following the topographic correction, the definitions are lost and this internal variability may be attributed to such factors as the age, canopy density, and amount of understory visible to the satellite sensor. These factors can contribute to spectral variability independent of topographically induced variation in the spectral reflectance properties of the deciduous forest classes. In contrast, the mixed deciduous appears to exhibit less internal variability in the shape of its cluster, but also undergoes the largest shift toward the beech forest following topographic correction. The cedar forest training areas that represent both high and low density stands, form a defined spectral group with high interclass variability from the deciduous cover types.

An analysis of the spectral views should also consider that training areas are often selected independent of whether or not training area represents only forest canopy reflectance, or also contains the reflectance signal from the secondary understory layers of the forest. In this study area, the impacts of the secondary understory may play a role of decreasing inter class variability for the younger birch and beech forest stands as they tend to form a more open forest canopy and are characterized by a dense bamboo understory layer. This understory layer may in fact be potentially masking differences between open canopy training areas where younger forest stands typically occur, creating class confusion.

3.4.2 Forest Classification Accuracy & Forest Cover Analysis

Land cover classification studies typically show that certain cover types achieve higher or lower classification accuracies than others (Congalton, 1991). The classification error matrix for the land and forest cover types is presented in Table 3.2. The forest cover types accuracies range from 77-89 %. Beech forest had the highest accuracy at 89 % followed by cedar at 82 %. Some confusion between the beech and birch cover types may exist, since the boundaries of these classes do not necessarily form clear bona-fide boundaries but rather grade together with the birch replacing the beech through natural regeneration (Kakubari, pers. Comm.).

The final classified classification of the forest and land cover classes is shown in figure 3.6. An analysis of the landscape structure metrics for the forest classes shows that beech forest dominates the landscape at 41%, followed by mixed deciduous (29.5%), birch (19%), anthropogenic/urban (5.1 %) and cedar forest classes (5.0 %). The total landscape area patch metric shows that both the beech and mixed deciduous forest classes have the largest numbers of forest patches that have the larger mean patch sizes in comparison to the other forest and land cover types following topographic correction (Table 3.3ab). Ski hills and cedar forest classes instead tend to occur as smaller patches. These patches are not forest fragments, however, rather they are classes that result from a physical land cover change that occurred the ski course was developed and the forest cover types were replanted.

In industrialized areas, forest and land cover classification accuracy should be assessed in the context of the complexities associated with a given class and in the context of the classifier. Although land and forest cover classification studies typically highlight certain forest cover types that exhibit higher classification accuracies, they are often not related to the inherent variability in the spectral reflectance properties of the forest cover types in the landscape. Forest cover types were affected by physical land cover changes (i.e replanting) achieved the highest classification accuracies compared to those classes that were altered by localize harvesting or thinning practices. The ability to detect and classify the cedar and anthropogenic classes increased, as they generally maintained a more bona-fide boundary and defined separability from those land and forest cover types that surrounded them. Urban areas tended to have much high spectral reflectance in comparison to the deciduous beech, birch and mixed deciduous forest cover types that are natural to the area tended to exhibit lower spectral contrast.

Therefore, the process of selecting training areas to represent a land cover type across a scene that are commonly conducted in non-industrialized flat areas may be less transferable to mountain areas that are affected by dynamic land use and cover change processes. Forest cover types that are viewed as merchantable timber resources, may for example exhibit higher variability in spectral reflectance within a study area than another forest cover types, which have no perceived merchantable value and are not disturbed. Therefore, knowledge of forest management practices

over local areas can be particularly important for the selection of training areas for satellite image based monitoring systems that attempt to use satellite imagery to classify forest cover across administrative boundaries undergoing difference forest harvesting practices.

3.4.3 Implications for Regional Monitoring Systems

Industrialized landscapes that have been affected by both natural and human alteration are the forested landscapes of the future. Although advances in satellite imaging system design may become available to analyze such areas in the future, increased spectral variability among land cover types may not be overcome by using conventional image classification techniques to process higher spatial resolution imagery (Hsieh *et. al*, 2001). LUCC studies using satellite imagery for classification and monitoring purposes (Adams, 1999) should be aware of the limitations when attempting to develop standardized vegetation classification schemes and image classification methodologies for regional/global forest cover mapping. As a result of variability in the spectral reflectance among different forest cover types, similar forest cover classification accuracies may not be achievable in industrialized landscapes as found in flat, less industrial areas. Assessing the spectral separability of the land cover types is key for determining what forest cover types can be suitably represented in a forest cover classification scheme.

It is not possible to provide a single solution to the challenges associated with mapping forest and land cover over both small and large areas. But, as satellite imagery is increasingly being used to make characterize forest cover and examine landscape changes, it is important to consider how LUCC processes can also affect the ability to detect and classify forest cover types using a given satellite imagery and image processing methodology. Improved methods for managing intra and inter class variability in the spectral response of forest cover types requires both a better understanding of the spatial and temporal spectral responses of the vegetation types. Further study into how both sensor related parameters (i.e. spatial resolution) and temporal issues (i.e. phenology) could be used to better quantify these two sources of variability. As a result of the high number of species that can occur in an area and the phenological changes to the forest cover types over a growing season, image classification methodologies will likely achieve high accuracy by optimizing satellite image acquisition dates to time periods where maximum separability can be achieved among forest cover species. In the case of Mt. Naeba, the optimal image acquisition date for the study areas will likely occur in the fall season where one or more tree species begins to senesce and change leaf color at different time periods.

3.5 CONCLUSION

This study suggests that the Jeffries Matusita distance and the n-dimensional visualizer tools can aid in assessing the ability to select adequate training areas pre and post image classification. The topographic correction can also be used to remove dominant topographic effects that shade land cover types adjacent to mountain areas. Such correction did not however eliminate the spectral variability that is inherent in those forest cover types training areas gathered in a landscape affected by prolonged forest harvesting and thinning disturbances. Both the JM distance and the n-dimensional viewing tools can be useful in developing or refining a forest cover classification legend for large scale mapping purposes. Overlapping spectral classes can be identified and pixels examined as to the location and cause of the variability for a given forest cover type. Both the topographic correction and measures of spectral separability should be assessed before using training areas selected in one area to generalize land cover types in another regions.

3.6 LITERATURE CITED

Adams, J. 1999. A suggestion for an improved vegetation scheme for local and global mapping and monitoring. *Environmental Management,* 23 (1), 1-13.

Becker. A & Bugmann, H. (Eds.) 2001 Global Change and Mountain Regions. *GTOS Report 28, IHDP Report 13.* IGBP Secretariat, Stockholm, 86 pp.

Congalton, R.G. 1991. A Review of Assessing the Accuracy of Classifications of Remotely Sensed Data. *Remote Sensing of Environment*, 7, 35-46.

Dale, V. 1997. The relationship between land-use change and climate change. *Ecological Applications*, 7 (3), 753-769.

Fahsi, A., Tsegaye, T., Tadesse, W., Coleman, T. 2002. Incorporation of digital elevation models with Landsat-TM data to improve land cover classification accuracy. *Forest Ecology and Management*, 128, 57-64.

Feng, J., Rivard, B., Sánchez-Azofeifa, G.A. 2003. Topographic normalization of hyperspectral data: implications for the selection of spectral end members and lithologic mapping. *Remote Sensing of Environment*, 85, 221 – 231.

Gruen, A. & Murai, S. 2002 Special Issue: Geomatics in Moutainous Areas—The international year of the Mountains 2002. *ISPRS Journal of Photogrammetry & Remote Sensing*, 57, 1-4.

Hsieh, P., Lee, L., Chen, N. 2001. Effect of Spatial Resolution on Classification Errors of Pure and Mixed Pixels in Remote Sensing. *IEEE Transactions on Geoscience and Remote Sensing*, 39 (12), 2657-2663.

Jansky, L., Ives, J.D., Furuyashiki, K., & Watanabe, T. 2002. Global mountain research for sustainable development. *Global Environmental Change*, 12, 231-239.

Kakubari, Y. 1977. Distribution of primary productivity along the altitudinal gradient. *J. Int. Biol. Program Synth*, 16, 201-212.

Kakubari, Y. 1987. Modelling the productive structure and function of natural forests of Fagus crenata at different altitudes in Naeba Mountains — An analysis of dry matter production with an eco-physiological computer simulation model based on an individual tree. *Bull. Tokyo Univ. For.*, 76, 107-162.

Kakubari, Y. 1991. Primary productivity for a Fifteen-Year Period in a Natural Beech *Fagus Crenata* Forest in the Naeba Mountains. *J. Jpn. For. Soc.*, 73 (5), 370-374.

Kira, T. 1949. Forest Zones of Japan. Ringyo Gijutsu Kyoukai, Tokyo and Sapporo, 41 pp. [In Japanese].

Kruse, F. A., Lefkoff, A.B., Boardman, J.W., Heidebrecht, K.B., Shapiro, A.T., Barloon, P.J. & Goetz, A.F.H. 1993. The Spectral Image Processing System (SIPS) -- Interactive Visualization and Analysis of Imaging Spectrometer Data. *Remote Sensing of Environment,* 44, 145-163.

Lambin, E.F, Turner, B.L., Geist, H.J., Agbola, S.B., Angelsen, A., Bruce, J.W., Coomes, O.T., Dirzo, R., Fischer, G., Folke, C., George, P.S., Homewood, K., Imbernon, J., Lemans, R., Li, X., Moran, E., Mortimer, M., Ramakrishna, P.S., Richards, J.F., Scans, H., Steffen, W., Stone,

G.D., Sedan, U., Beldam, T.A., Vogel, C. & Up, J. 2001. The causes of land-use and land-cover change: moving beyond the myths. *Global Environmental Change*, 11, 261-269.

Maruyama, K. 1971. Effect of altitude on dry matter production of primeval Japanese beech forest communities in Naeba Mountains. *Mem.Fac. Agr. Niigata Univ*, 9, 85-171.

Maruyama, K. 1977. Beech forests in the Naeba Mountains. *J-IBP Synthesis,* 16, 186-212.

Masek, J. G., Honzak, M., Goward, S.N., Liu, P., Pak, E. 2001. Landsat-7 ETM+ as an observatory for land cover: Initial radiometric and geometric comparisons with Landsat-5 Thematic Mapper. *Remote Sensing of Environment,* 78, 118-130.

Matsushita, B. & Masayuki, T. 2002. Integrating remotely sensed data with an ecosystem model to estimate net primary productivity in East Asia. *Remote Sensing of Environment*, 81, 58-66.

McGarigal, K. & Marks, B. 1994. FRAGSTATS*ARC: Spatial pattern analysis program for quantifying landscape structure (Version 2.0). Corvallis, OR.

Proy, C., Tanre, D., and Deschamps, P. Y., 1989. Evaluation of Topographic effects in remotely sensed data. *Remote Sensing of the Environment*, 30, 21-32.

Richards, J.A. 1994. Remote sensing digital image analysis. Berlin: Springer-Verlag (281pp).

Richter, R. 1998. Correction of satellite imagery over mountainous areas. *Applied Optics*, 37 (18), 4004 – 4015.

Sánchez-Azofeifa, G. A., Kachmar, M.A, Kalácska, M. & Hamilton, S. 2003. Experiences in Field Data Collection for Land Use and Land Cover Change Classification in Boreal and Tropical Environments. *In Methods for Remote Sensing of Forests: Concepts and Case Studies.* Kluwer Academic Publishing pp.433 – 446.

Sousa, W.P. 1984. The Role of Disturbance in Natural Communities. *Annual Review of Ecology and Systematics,* 15, 353-391.

Welch, R. Madden, M. & Jordan, T. 2002. Photogrammetric and GIS techniques for the development of vegetation databases of mountainous areas: Great Smoky Mountains National Park. *ISPRS Journal of Photogrammetry and Remote Sensing*, 57, 53-68.

Yamada, M., & Maruyama, K. 1962. Studies on the production structure of forest: Primary productivity of *Fagus crenata* in plantation. *J. Jap. For. Soc,* 51, 331-339.

Zukowskyj, P.M., Bussell, M.A., Power, C., & Teeuw, R.W. 2001. Quantitative accuracy assessment of contextually filtered classified images. *International Journal of Remote Sensing*, 22, 16, 3203-3222.

Table 3.1. Jeffries-Matusita distance calculated on the original and topographically corrected image for the four forest cover types over Mt. Naeba in the central part of Honshu, Japan.

Original Image		Topo-Corrected Image	
Cover Types	J-M	Cover Types	J-M
Cedar & Beech	1.99	Cedar & Beech	1.99
Cedar & Birch	1.99	Cedar & Birch	1.99
Cedar & Mix D.	1.98	Cedar & Mix D.	1.98
Birch & Mix D.	1.99	Birch & Mix D.	1.98
Mix D. & Beech	1.92	Mix D. & Beech	1.34
Beech & Birch	1.69	Birch & Beech	1.74

Table 3.2 Error Matrix for the land cover classes on the topographically corrected image on the Mt. Naeba study area, Japan.

Land & Forest Classes	Validation Points							
	Beech	Cedar	Birch	Mix Dec.	Water	Anthro	Total	%
Beech	16		1	1			18	89
Cedar		18	2	2			22	82
Birch	2		10	1			13	77
Mix Dec.			1	4			5	80
Water					1		1	100
Anthro						10	10	100
							69	
Total	18	18	14	8	1	10		86
Percentage (%)	89	100	71	50	100	100		Overall Accuracy

Table 3.3a Land cover type as a percentage of total land cover area within the Naeba mountain study area.

Metrics	Anthro	Beech	Birch	Mix Decid	Cedar
% of total landscape	**5.1**	**41.0**	**19.0**	**29.5**	**5.0**
Class Area (ha)	493	3963	1833	2856	483
Number Patches	165	500	1286	937	321
Mean Patch Size (ha)	448	3747	1211	2477	400

Table 3.3b Land cover type as a percentage of total land cover area within the Naeba mountain study area without topographic correction.

Metrics	Anthro	Beech	Birch	Mix Decid	Cedar
% of total landscape	**6.3**	**45.8**	**19.2**	**23.4**	**5.0**
Class Area (ha)	603	4428	1857	2263	479
Number Patches	226	465	1108	778	213
Mean Patch Size (ha)	525	4236	1236	1812	412

Figure 3.1 Location of the study area, central part of Honshu, Japan.

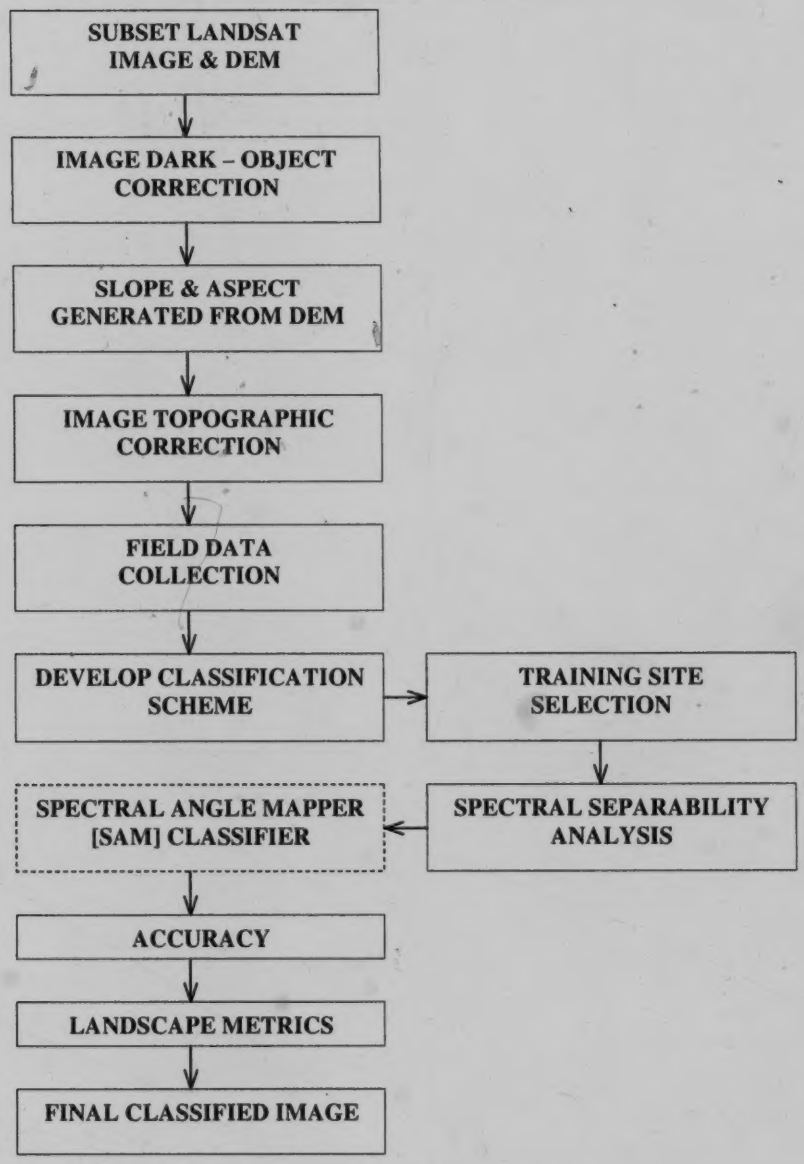

Figure 3.2 Flowchart of the processes involved in pre-processing and classifying the Landsat TM imagery for Mt. Naeba in the central part of Honshu, Japan. A cloud free 6-channel multispectral Landsat TM 5 (Path 108/Row 34) image was acquired over Mt. Naeba on September 01, 1999 at a solar azimuth of 121^0 and 59^0 sun angle elevation

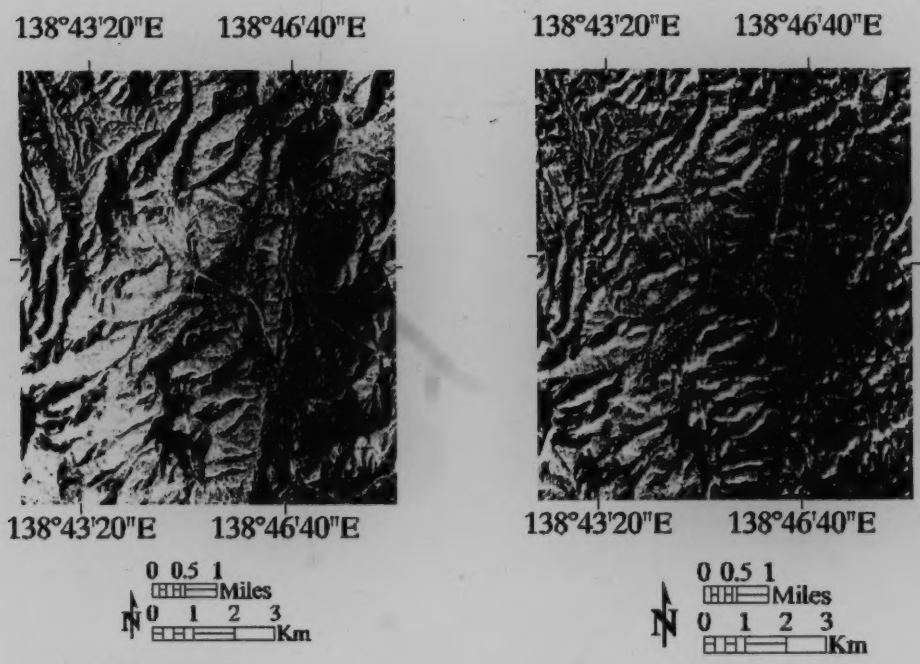

Figure 3.3 a) Original LANDSAT TM 5 color composite (bands 543 as RGB) over Mt. Naeba and b) Topographically corrected 3-Band Image Composite (Bands 5 4 3) of the LANDSAT TM 5.

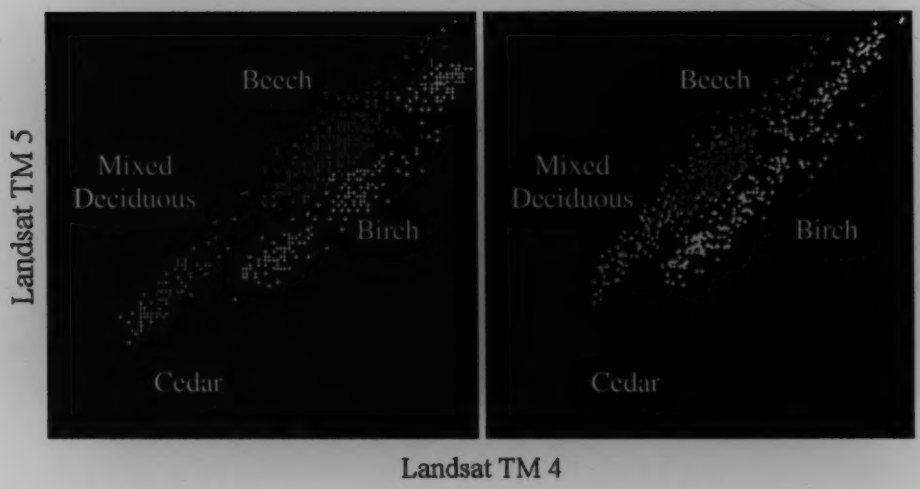

Figure 3.4. Two - dimensional scatter plot of training site spectral data for forest classes within the Mt. Naeba study area in the Central part of Honshu, Japan a) pre topographic correction Birch Forest (Yellow), Beech (Green), Cedar (Red), Mix Deciduous (Cyan) & b) post topographic correction. Spectral data displayed in Landsat TM bands 4 & 5.

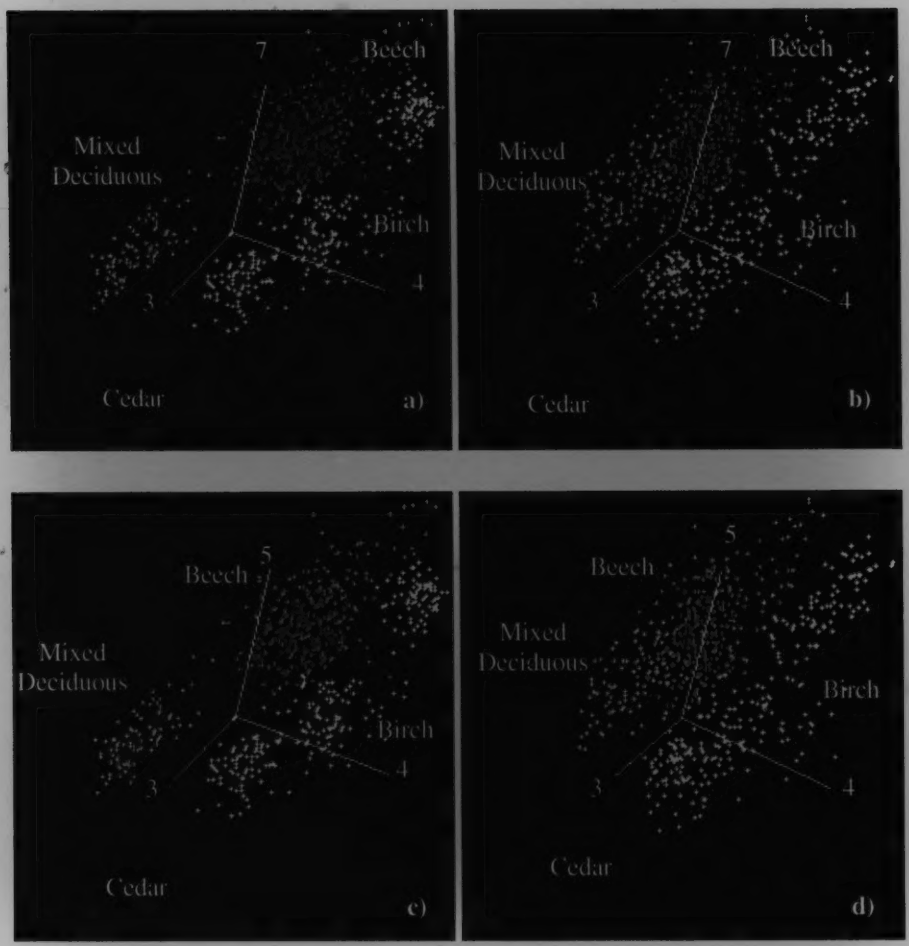

Figure 3.5 *n*-Dimensional Visualization of training site spectral data for the classes of interest within the Mt. Naeba study area in the central part of Honshu, Japan a) and c) pre topographic correction & b) and d) post topographic correction. Birch (Yellow), Beech (Green), Cedar (Red), Mix Deciduous (Cyan). Displayed axis refers to Landsat TM bands.

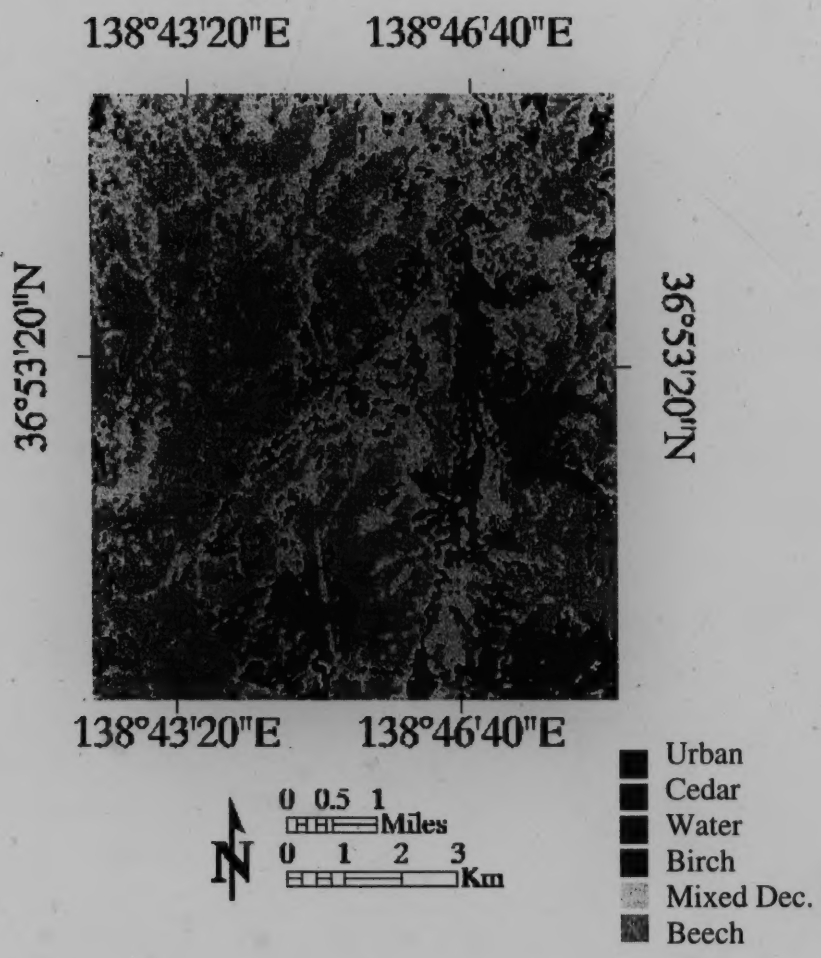

Figure 3.6 Spectral angle mapper (SAM) classification of the Landsat TM image acquired over Mt. Naeba in the Central part of Honshu, Japan.

CHAPTER 4

SUMMARY & CONCLUSIONS

4.1 SUMMARY & CONCLUSIONS

This thesis has explored the use of medium and high-resolution multispectral satellite imagery to detect, classify and analyze forest cover in two forest ecoregions. The first study (Chapter 2) focused on detecting and analyzing post-fire *residual* forest islands within the perimeter of two fires that occurred in the boreal forest of Northern Alberta, Canada (2001 Chisholm and 2002 House River Fire). The second study (Chapter 3) employed Landsat TM 5 satellite imagery to classify forest cover types on the highly industrialized temperate Naeba Mountains, which are located in the central part of Honshu, Japan. This chapter summarizes the major findings from Chapter 2 and 3 of this thesis and provides recommendations for the use of multispectral satellite imagery for regional forest and land cover mapping and monitoring.

Chapter 2: Detection and Analysis of Post-Fire Residual Forest Islands Using Medium and High-Resolution Satellite Imagery

Forest fires can kill many trees in a forested area, but unburnt residual forest islands also remain alive within the fire perimeter. Using medium and high-resolution satellite imagery, live residuals could be isolated and classified from non-target cover types with > 88 % accuracy using both unsupervised-masking and supervised image classification

techniques. Grouping residuals into nine MMU classes shows that within the fire perimeter smaller MMU classes contain the highest numbers of residual patches, but larger MMU classes contain the largest amount of residual forest. Residual tend to exist as more complex shapes at smaller MMU classes with the most complex shapes occurring in the higher resolution IKONOS satellite imagery. This study suggests that although remote sensing techniques can improve estimates of the amount of forest burnt by fires, the choice of satellite imagery used and the spectral contrast of the target, size of MMU chosen and extent of linear feature disturbances impacts the size, number and shape of residual patches within fire perimeters. The results serve as important lessons for forest managers that aim to retain green areas in their forest management agreement areas in an attempt to emulate fire patterns in the landscape.

Chapter 3. Forest Cover Classification in Industrialized Mountain Terrain Using Landsat TM 5

The Jeffries-Matusita distance and the *n*-dimensional visualizer tools can aid in assessing the ability to select training areas to represent the forest cover types within a topographically complex industrialized landscape. Although a cosine lambertian topographic correction aims to improve separability between different cover types, such a correction cannot eliminate the spectral variability inherent in forest cover types that occur in areas affected by prolonged forest harvesting and thinning disturbances. The Jeffries-Matusita distance highlights forest cover classes with lower separability that is critical in developing or refining a forest cover classification legend for accurate forest

cover mapping purposes. The Jeffries-Matusita distance measure allowed for the comparison of separability that can be used to refine the classification legend and aid in choosing representative training areas for a forest cover type. This study suggests that regional and global monitoring systems using satellite imagery for monitoring purposes should recognize the limitations of using forest cover training areas to represent forest cover types across a scene in landscape where both natural (i.e. topography) and anthropogenic (i.e. forest harvesting) impact the structure of the forest canopy. These results have implications for regional monitoring systems that often acquire and use medium resolution satellite imagery to classify land cover over areas in areas where dynamic land use and cover change processes are occurring.

4.2 RECOMMENDATIONS

- In post fire studies, it is recommended to optimize the choice of satellite image used for investigating a fire-affected area to the level of landscape detail required to provide forest management decisions. The choice of sensor, MMU and impact of linear features affect residual metrics and should therefore be considered in future investigation of post fire residuals with sensors that have higher spatial and spectral imaging capabilities.

- In the Mt. Naeba study area, it is recommended to acquire images at times where the spectral contrast between forest cover types can be maximized due to phenological changes to the forest. If cloud cover does not affect the selection of

an image, an image should be acquired during the fall season where the spectral contrast between the deciduous forest cover types is increased. In the middle of the summer season, the spectral differences between the beech, birch and mixed deciduous canopies are sufficiently lowered, reducing the separability between these forest cover types.